OXFORD UNIVERSITY PRESS Cerebral Cortex

Absence of LPA_1 signaling results in defective cortical development

Journal:	*Cerebral Cortex*
Manuscript ID:	CerCor-2007-00088.R1
Manuscript Type:	Original Articles
Date Submitted by the Author:	07-Jun-2007
Complete List of Authors:	Estivill-Torrús, Guillermo; Fundación Imabis, Hospital Carlos Haya, Unidad de Investigación Llebrez-Zayas, Pedro; Fundación Imabis, Hospital Carlos Haya, Unidad de Investigación Matas-Rico, Elisa; Fundación Imabis, Hospital Carlos Haya, Unidad de Investigación Santín, Luis; Universidad de Málaga, Facultad de Psicología, Departamento de Psicobiología y Metodología de las Ciencias del Comportamiento Pedraza, Carmen; Universidad de Málaga, Facultad de Psicología, Departamento de Psicobiología y Metodología de las Ciencias del Comportamiento De Diego, Isabel; Universidad de Málaga, Facultad de Medicina, Departamento de Anatomía y Medicina Legal Del Arco, Ignacio; Fundacion Imabis, Hospital Carlos Haya, Unidad de Investigacion Fernandez-Llebrez, Pedro; Universidad de Málaga, Facultad de Ciencias, Departamento de Biología Celular, Genética y Fisiología Chun, Jerold; Helen L. Dorris Child and Adolescent Neuropsychiatric Disorder Institute, The Scripps Research Institute, Department of Molecular Biology Rodriguez de Fonseca, Fernando; Fundación Imabis, Hospital Carlos Haya, Unidad de Investigación
Keywords:	brain development, cerebral cortex, LPA, lysophosphatidic acid, neurogenesis

Section: Genetic /Molecular /Development

Title: Absence of LPA_1 signaling results in defective cortical development

Authors and author addresses:

Guillermo Estivill-Torrús[1], Pedro Llebrez-Zayas[1], Elisa Matas-Rico[1], Luis Santín[2], Carmen Pedraza[2], Isabel De Diego[3], Ignacio Del Arco[1], Pedro Fernández-Llebrez[4], Jerold Chun[5] and Fernando Rodríguez De Fonseca[1].

(1) Unidad de Investigación, Fundación IMABIS, Hospital Carlos Haya, Avenida Carlos Haya 82, E-29010 Málaga, Spain

(2) Departamento de Psicobiología y Metodología de las Ciencias del Comportamiento, Facultad de Psicología, Universidad de Málaga, Campus de Teatinos, E-29071, Málaga, Spain

(3) Departamento de Anatomía y Medicina Legal, Facultad de Medicina, Universidad de Málaga, Campus de Teatinos, E-29071, Málaga, Spain

(4) Departamento de Biología Celular, Genética y Fisiología, Facultad de Ciencias, Universidad de Málaga, Campus de Teatinos, E-29071, Málaga, Spain

(5) Department of Molecular Biology, Helen L. Dorris Child and Adolescent Neuropsychiatric Disorder Institute, The Scripps Research Institute, 10550 North Torrey Pines Road, ICND 118, La Jolla, California 92037, USA.

Corresponding author: Guillermo Estivill-Torrús

Unidad de Investigación, Fundación IMABIS, Hospital Carlos Haya, Pabellón A, planta 7ª, Avenida Carlos Haya 82, E-29010 Málaga, Spain. Tel: +34 951 290 346. Fax: +34 951 291 447. Email: guillermo.estivill@fundacionimabis.org.

running title: Corticogenesis in mice lacking LPA_1 signaling

Number of figures and tables: Figures: 8; Tables: 1; Supplementary figures: 4; Supplementary Tables: 2

Number of pages: 36

Key words: brain development, cerebral cortex, LPA, lysophosphatidic acid, neurogenesis.

Abstract

Lysophosphatidic acid (LPA) is a simple phospholipid with extracellular signaling properties mediated by specific G protein-coupled receptors. At least two LPA receptors, LPA_1 and LPA_2, are expressed in the developing brain, the former enriched in the neurogenic ventricular zone, suggesting a normal role in neurogenesis. Despite numerous studies reporting the effects of exogenous LPA using in vitro neural models, the first LPA_1 loss-of-function mutants reported did not show gross cerebral cortical defects in the 50% that survived perinatal demise. Here we report a role for LPA_1 in cortical neural precursors resulting from analysis of a variant of a previously characterized LPA_1-null mutant that arose spontaneously during colony expansion. These LPA_1-null mice, termed maLPA_1, exhibit almost complete perinatal viability and show a reduced ventricular zone, altered neuronal markers, and increased cortical cell death that results in a loss of cortical layer cellularity in adults. These data support LPA_1 function in normal cortical development, and suggest that the presence of genetic modifiers of LPA_1 influences cerebral cortical development.

Introduction

Development of the cerebral cortex requires a carefully coordinated sequence of events essential for the construction of a functional brain. Cortical cells arise mainly in the ventricular zone (VZ), a pseudostratified neuroepithelium of dividing neural progenitor cells (NPCs) lining the surface of the telencephalic lateral ventricles (Sidman and others 1959; Bayer and Altman 1991). The cortical layers form in an inside-out sequence by migration of neurons in coordination with proliferative processes (Takahashi and others 1999), including influences of cleavage planes and programmed cell death (Blaschke and others 1996, 1998). Consequently, any alteration in this sequence of events could have a critical impact on normal brain development (Caviness and others 1995; Rakic and others 1995).

Neurogenesis is influenced by numerous factors including intrinsic mechanisms and extracellular signals such as growth factors (Reynolds and others 1992; Jin and others 2002; Qian and others 1997). Of these, lysophospholipids have recently emerged as important influences on normal nervous system development (Chun and others 2002; Anliker and Chun 2004; Chun 2005; Gardell and others 2006). Lysophosphatidic acid (LPA) is a prominent endogenous lysophospholipid that can act as an extracellular signal through specific G protein-coupled receptors, five of which have been identified, $LPA_{1\text{-}5}$ (Anliker and Chun 2004; Chun and others 2002; Ishii and others 2004; Lee and others 2006). LPA_1 was identified in the embryonic cortex, enriched in the VZ. LPA_1 and LPA_2 show spatio-temporally regulated gene expression, suggesting a role in regulation of cortical neurogenesis (Hecht and others 1996; Contos and Chun 2001; Anliker and Chun 2004). Previous studies have demonstrated cortical functions for LPA receptors via exogenous delivery of LPA inducing morphophysiological changes in postmitotic neurons and cortical NPCs (Dubin and others 1999; Lu and others 1999; Fukushima and others 2000, 2002; Fujiwara and others 2003; Dash and others 2004; Fukushima 2004).

LPA exposure in an ex vivo cortical culture increases NPC terminal mitosis, inducing cortical folding and thickening, effects which depend on LPA_1 and LPA_2 expression (Kingsbury and others 2003, 2004). Receptor loss-of-function studies using LPA_1-null or LPA_1/LPA_2-double null mice have demonstrated ~50% perinatal lethality and, amongst survivors, behavioral deficits that suggest centrally mediated defects (Contos and others 2000, 2002; Harrison and others 2003). These mice are smaller, exhibit cranial dysmorphism and have increased apoptosis in the sciatic nerve (Contos and others 2000, 2002; Kingsbury and others 2003; Anliker and Chun 2004). Somewhat surprisingly, only minor abnormalities were observed in mutant cerebral cortices, with the exception of a variable reduction in embryonic cerebral wall thickness (Contos and others 2000).

During propagation of the original mixed background strain of LPA_1-null mice (Contos and others 2000) in our laboratories, a spontaneous, stable variant arose and led to the establishment of the LPA_1-null reported here as the "*Malaga* variant" (here referred to as "maLPA_1-null" mice). We show that their LPA_1 absence results in defects in cortical development including a reduction in proliferative populations, premature NPC maturation, and increased apoptosis. The observed alterations not only affected NPCs but also resulted in reduced adult cortical cellularity.

Material and methods

Mice

Procedures were carried out with wild-type and maLPA_1-null heterozygous and homozygous females (on a mixed background C57Bl/6 × 129SW) in compliance with European animal research laws (European Communities Council Directive 86/609/EEC and 2003/65/CE). A spontaneously established LPA_1-null mouse colony, termed maLPA_1-null (from *Málaga variant of* LPA_1-null) was derived from previously reported (Contos and others 2000) during the original colony expansion by crossing heterozygous foundation parents within their original mixed background. More than twelve maLPA_1-null generations have been obtained

exhibiting all the defects described in this work. MaLPA$_1$-null mice carrying an *lpa*$_1$ deletion were born at the expected mendelian ratio and survived to adulthood exhibiting increased perinatal survival rates and absence of suckling defects when compared with original LPA$_1$-null mice (Supplementary Tables 1, 2 and Supplementary Fig. 1).

For experiments, the day of the vaginal plug following mating was designated embryonic day 0.5 (E0.5). Research was performed on E11.5, E14.5, E15.5, E16.5, E18.5 embryos, perinatal pups (postnatal day 0 to P7) and 12 week-old male mice always obtained from heterozygous x heterozygous/homozygous maLPA$_1$-null mating and genotyped for *lpa*$_1$ deletion by PCR (Contos and others 2000; see Supplementary Fig. 2). LPA$_1$ absence was also confirmed by immunohistochemistry on embryonic cerebral cortices (Supplementary Fig. 2).

Immunohistochemistry

Experiments were performed from E11.5 to neonatal stages. At least twelve embryos from each age per genotype were used. Brains were dissected out into cold phosphate buffer, fixed in Bouin's solution overnight at room temperature, washed and embedded in paraffin. All steps were carried out at room temperature. Sections (10µm) were first treated for 10 min with 0.1 M phosphate buffered saline pH 7.4 (PBS) containing 10% methanol and 10% hydrogen peroxide to inactivate endogenous peroxidase. After washing, they were exposed to anti-PCNA (Sigma, St.Louis, MO), anti β-tubulin-III (Promega Co., Madison, WI), anti-GAP43 (Sigma) mouse monoclonal or anti-phospho-histone-H3 (Upstate, Lake Placid, NY), anti-parvalbumin (Swant, Bellinzona, Switzerland), anti-Tbr2 (Abcam, Cambridge, UK) and anti-LPA$_1$ (Affinity Bioreagents, Golden, CO) rabbit polyclonal antibodies for 18h. Standardized detection used biotin-conjugated rabbit anti-mouse or swine anti-rabbit (as appropriate) immunoglobulins (DakoCytomation, Glostrup, Denmark), ExtrAvidin®-peroxidase (Sigma) and DAB (Sigma). All the antibodies were used according to the manufacturer's instructions and diluted in PBS containing 0.5% Triton X-100 and normal serum (rabbit or

swine serum, depending on the source of the secondary reagent used). Omission of the primary antibody resulted in no detectable staining. Sections were counterstained with hematoxylin when required. Parallel sections of some brains were stained with hematoxylin-eosin for a general histological description.

For the analysis of phospho-histone-H3 positive cells, four sections per embryo and eight embryos for each genotype were analyzed and at least 200 cells in the proliferative VZ/SVZ zones in each sectioned brain were assessed. At each section, cells were estimated from a 150 μm x 150 μm bin comprising the cortical VZ/SVZ. Percentages were expressed from the total hematoxylin counted cells.

In situ hibridization

In situ hibridization was carried out on E14.5 embryos. At least eight embryos per genotype were used. Brains were dissected into cold phosphate buffer and fixed overnight in 4% paraformaldehyde at 4ºC and kept at 4°C until dehydration in methanol/PBT (PBS with 0.1% Tween-20). After rehydration, the telencephalon was embedded in a gelatin/albumin mixture and cut 200 μm thick sections with a vibro-slicer (Campden Instruments, Loughborough, UK). Finally, they were dehydrated in methanol/PBT and kept at -20°C overnight. In situ hibridization used a digoxygenin-labeled riboprobe transcribed from a *Pax-6* cDNA clone (kind gift from D. Price, University of Edinburgh). TAG-1 (kindly provided by M. Wassef, Ecole Normale Superieure, Paris and D. Karagogeos, University of Crete) (see Supplementary Fig. 4) was produced as previously described (Denaxa and others 2001). Probes were labeled with digoxigenin-UTP using commercial kits (Roche, Mannheim, Germany; Promega) and hybridization was performed at 70ºC, using a water bath, on previously rehydrated sections. An anti-digoxigenin alkaline phosphatase-conjugated antibody (Roche; 1:2000) and NBT/BCIP (Roche) were used for probe detection.

Cortical precursor cultures

NPCs from E14.5 cortices were enzymatically dissociated by incubation for 45 min at 37°C in Earle's buffered salts solution containing 20 units/ml papain (Papain Dissociation System, Worthington Biochemical,

Lakewood, NJ) and cultured as described by Estivill-Torrus (Estivill-Torrús and others 2002). Briefly, cells in suspension were plated onto poly-L-lysine-coated wells (LabTek II™, Nunc, Rochester, NY) at a density of 1.5 x 10^5 cells /cm^2 and cultured in serum-free Dulbecco's modified Eagle's medium (Sigma) at 37ºC and 5% CO_2.

Cultures were analyzed at various times after plating (12.75-24 hours, see below) and each time-point was repeated in four separate experiments. Viable cells were identified on the basis of morphology and Trypan Blue exclusion. For cell counts, 800-1500 viable cells per culture were assessed in six randomly selected microscope fields. Eight embryos were used per genotype.

To obtain the labeling index, twelve hours after plating, bromodeoxyuridine (BrdU) was added to the culture medium (final concentration 10μM) for 45 min and then removed and fresh culture medium added. Cells were fixed in 4% paraformaldehyde either immediately after the pulse of BrdU, i.e. 12.75 hours after plating, or at 18, 24, and 36 hours after plating, and processed as formerly reported (Estivill-Torrús and others 2002). Detection of BrdU utilized a monoclonal anti-BrdU antibody (Sigma). Immunocytochemistry was carried out at room temperature as follows. Cultures were treated with 90% methanol prior to incubation in blocking solution (PBS containing 0.5% Triton X-100 and 2.5% normal rabbit serum). Cells were then exposed to the primary antibody for 18 hours and subsequently processed with biotin-conjugated rabbit anti-mouse Ig (Dako) and ExtrAvidin®-peroxidase (Sigma). Reactions were visualized with DAB (Sigma).

Other immunocytochemical reactions were performed similarly using anti-$p27^{kip1}$ (BD Biosciences, Franklin Lake, NJ), anti-PCNA (Sigma), anti-Cyclin A (Sigma), anti-β-tubulin-III (Promega), anti-MAP2 (Sigma), anti-GFAP (Sigma) or anti-CNPase (Sigma) monoclonal antibodies. All primary antibodies were diluted in blocking solution. For dual-labeling experiments, cultures were processed for the second staining using alkaline phosphatase conjugated rabbit anti-mouse, following standard procedures and visualized with NBT/BCIP (Roche). Percentages of labeled cells were expressed from the total cells as identified by phase contrast or histological conventional staining. Cell death was also analyzed using a DeadEnd™ Fluorometric Apoptosis Detection System (Promega) following the manufacturer's instructions.

BrdU labeling for the analysis of migration patterning

Pregnant dams were given a single injection of BrdU (70 µg /g in sterile saline i.p.) on E14.5. Embryos were removed 45 minutes and 12h later or on E18.5. After dissection, brains were fixed overnight in 4% paraformaldehyde at 4ºC, embedded in wax, serially sectioned coronally at 10 µm, mounted and immunoreacted to reveal BrdU labeling, as described (Gillies and Price 1993). BrdU cells were sorted into densely labeled cells, in which more than half of the nucleus is labeled, and lightly labeled cells, which have lighter nuclear labeling, indicating they had undergone more than one round of division after labeling. Telencephalic wall was analyzed in depth in non-adjacent coronal sections taken at the middle cortical portion. At each section, 100 µm wide radial strips were divided into different bins corresponding to cortical layering (see Fig. 5) and the position of each labeled cell assigned to a bin to generate histograms of average cell density against depth. The estimations combined results from eight sections per embryo and eight embryos per genotype. In each bin, the number of labeled cells is expressed as a percentage of the total number of labeled cells in the strip and means were compared statistically.

Western-blot analysis

Eight embryos per genotype were decapitated and telencephalic hemispheres dissected out and frozen sectioned. After scraping out layer I, upper and middle regions comprising cortical layer II/III were accurately dissected and homogenized in lysis buffer containing 10mM Tris-HCl, 1 mM EDTA, 250 mM sucrose, 1mM phenylmethylsulphonyl fluoride, 1 µg/ml leupeptin, 1 µg/ml aprotinin, 1 µg/ml pepstatin, pH 7.4. The homogenate was centrifuged for 10 min at 900 x *g* and the supernatant spun for 20 min at 75000 x *g*. The pellet was resuspended in the lysis buffer containing 1% Triton X-100 and subsequently centrifuged for 10 min at 14000 x *g* to eliminate the insoluble material. Samples containing 25 µg of protein determined by Bradford reactive (Sigma) were loaded in Laemli buffer and separated on 10% SDS-polyacrylamide gel by

electrophoresis. Proteins were electrotransferred to PVDF membranes at 100V for 1h. Non-specific binding was blocked by 1h incubation in PBS containing 5% non-fat dry milk and 0.1% Tween-20. Membranes were then exhaustively washed in PBS and incubated overnight at 4ºC in mouse monoclonal anti-GAP43 (Sigma) diluted in blocking buffer. Immunoreaction was visualized with standard procedures using a biotin-labeled rabbit anti-mouse antibody, ExtrAvidin®-peroxidase (Sigma) and 4-cloronaftol. Omission of the primary antibody resulted in no specific staining. Optical density measurement for each band was estimated using OptiQuant v.4.00 software (Packard Instruments Co. Downers Grove, IL) after membrane scanning.

Apoptosis detection

Estimation of apoptosis was performed for E11.5 embryos and P7 mice. Mice (eight per genotype and age) were transcardially perfused in 4% paraformaldehyde. Brains were dissected out, fixed overnight in the same solution at 4ºC, and cryosectioned. Coronal cortical sections of 30 µm were obtained and mounted onto poly-L lysine treated slides. Cell death was detected using a DeadEnd™ Fluorometric Apoptosis Detection System (Promega) following the manufacturer's instructions. Counterstain used ethidium bromide and cell number estimations were measured on non-adjacent coronal sections from the middle cortical portion according to the cited bin scheme.

Stereological studies

The numerical density of neurons in the primary motor cortex of 12-week old mice was determined by the optical disector method. Six animals per genotype were transcardially perfused with 4% paraformaldehyde and brains dissected out and overnight fixed at 4ºC. Analysis was performed on free-floating cryosections immunostained for a monoclonal mouse anti-NeuN (Chemicon, Temecula, CA) in accordance with the mentioned protocol, with minor modifications. After mounting, seven sections of 30 µm equally spaced along the rostral-to-caudal primary motor cortex extension were used per animal. Cortical layers were delineated according to the criteria of Paxinos and Flanking. A random set of 25-70 sampling optical disectors was

generated for each layer on each section using the C.A.S.T. Grid (Olympus). Each optical disector was a 43.4 µm x 43.4 µm sampling frame with exclusion lines. Counting was set starting at 5 µm below the surface and considering focused labeled neurons through the 15 µm section optical plane. The number of cells per unit of volume (*N*v) was calculated for each animal, as the number of applied disectors multiplied by Vdis; Vdis = Sd x Hd, where Sd = area of the disector grid (counting frame) and Hd = depth of disector. Data were analyzed statistically.

Mice sample size, statistical analysis and image acquisition

Most experiments used at least eight embryos per stage and genotype. No significant differences were found using different or same litters. Histological and densitometric analyses were tested for significance using the Student *t*-test. Stereological studies were analyzed using Kruskal-Wallis One-Way Analysis of Variance on Ranks and compared by post hoc analysis. In vitro data were compared by ANOVA (significance assigned when $P<0.05$). Immunostaining and fluorescence were analyzed under an Olympus BX51 microscope equipped with UPLSAPO x4 0.16 NA, x10 0.4 NA, x20 0.75 NA, x40 0.90 NA or x100 1.40 NA objectives and an Olympus DP70 digital camera. B/W image of cultured NPCs was acquired using a Canon Powershot digital camera coupled to a Leica DM IL inverted microscope equipped with x10 0.20 NA or x40 0.50 NA objectives. All pictures were analyzed using Adobe-Photoshop 7.0 software without modifying the content of the micrograph.

Results

Absence of LPA_1 generates anomalous cortical proliferative patterning

In the original LPA_1-null mice, exon 3, which contains the majority of the coding region of the murine *lpa*$_1$ gene, is completely deleted (Contos and others 2000). In accordance with their origin, maLPA_1-null mice show reduced size and body mass, craniofacial defects, including shorter snouts and wider-spaced eyes, and

reduced brain volume and mass (Fig. 1, *A-D*). Likewise, maLPA$_1$-null mice cortical NPCs did not cluster in vitro after addition of LPA as wild type (Fig. 4, *A*).

MaLPA$_1$-null mice reaching adulthood showed olfactory bulbs that were reduced in size compared with wild-type littermates and detectable changes in the shape of the cerebral hemispheres, appearing more compact and spherical (Fig. 1*C*). The gross morphology of subcortical structures, including the brainstem and cerebellum, were comparatively unaffected. Further analysis of the cortex of maLPA$_1$-null mice at different developmental ages revealed additional abnormalities that had not previously been described in the original LPA$_1$-null. By E18.5, wild-type and maLPA$_1$-null mice could be distinguished based on gross structure of brain and snout (Fig. 1*E*). Coronal sections of E18.5 embryos demonstrated a slight reduction in brain size and cortical thickness (Fig. 1*F*) that by P0 appeared as a more condensed cortex with somewhat diffuse boundaries between different layers (Fig. 1*G*). Mutant cortices displayed a marked reduction in layer width and an altered cellularity, particularly at deeper levels. In some cases, disturbances in the cortical surface could be observed (arrow in Fig. 1*G*).

During brain development, expression of LPA$_1$ is enriched in the ventricular zone synchronized with the neurogenic period (Hecht and others 1996), and gain-of-function studies have shown NPCs are responsive to LPA signaling. To determine whether cortical defects in maLPA$_1$-null mice involve deficiencies in normal proliferation of NPCs, we analyzed neuronogenic parameters in the cortex from the start of cortical neurogenesis at E11.5 through the closing stages at E18.5 (Caviness and others 1995). Immunostaining was performed using antibodies specific to proliferating cell nuclear antigen (PCNA), present in continually cycling NPCs (Ino and others 2000) and to neuron-specific class III beta-tubulin, an early indicator of postmitotic neuronal differentiation (Menezes and others 1994).

During early corticogenesis, the wild-type cerebral wall was composed almost entirely of PCNA-labeled NPCs forming the germinative VZ (Fig. 2*A,G*). Mature neurons reached the upper level to form the initial preplate consisting of a thin layer of tangentially oriented cells and fibers, together with the radially-oriented processes of underlying VZ cells (Fig. 2*B,J*). At this stage, maLPA$_1$-null embryos displayed a minor reduction of PCNA expression (Fig. 2*E,I*) and, most significantly, early and ectopic expression of class III beta-tubulin in the VZ, including some cells lining the ventricular surface (Fig. 2*F,L*). By E14.5 the developing wild-type cortex had a laminar structure comprising the proliferative layers (ventricular zone, VZ, and subventricular zone, SVZ), an intermediate zone (IZ) and the cortical plate (CP) containing differentiating neurons. Similarly, coronal sections of E14.5 wild-type brain showed a telencephalic wall delineated by PCNA-labeled NPCs forming the germinative layer (Fig. 2*M,S*) and a complementary upper layer of cells expressing neuronal beta-tubulin forming the IZ/CP levels (Fig. 2*N,V*). By contrast, and corresponding to the above observations, maLPA$_1$-null mice had a clearly smaller cortex by E14.5 and displayed a strongly reduced PCNA expression (Fig. 2*Q,U*). The reduction of the proliferative area was coupled with a proportional increase in beta-tubulin-III expression (Fig. 2*R,X*). Furthermore, most maLPA$_1$-null NPCs showed increased numbers of beta-tubulin-III positive cells in the putative VZ/SVZ, and many atypical fibers above this region running parallel to the ventricular surface (arrow and arrowhead, respectively, in Fig. 2*X*). Heterozygous embryos showed a graded pattern of immunostaining between that observed for wild-type and homozygous genotypes (see middle column in Fig. 2). Defects in cortical proliferation/differentiation patterning affected, in similar terms and proportions, both cerebral hemispheres throughout the rostral-caudal axis and including the olfactory bulb. Further analysis of mitotic activity was performed using an antibody against the phosphorylated form of histone H3 (anti phospho-H3) that identifies mitotic chromosome condensation (Hendzel and others 1997). Phospho-H3 immunolabeling at E14.5 revealed a marked decrease (32%) in the number of mitotic VZ cells in the maLPA$_1$-null cortices, as compared to wild-type controls (P=0.01; Fig. 3*A, B*) that correlated with the reduction in the proliferative PCNA-stained population. Parallel analysis of abventricular mitosis in SVZ showed similar reduced phospho-H3 immunolabeling in the absence of LPA$_1$

(Fig. 3*B*). No ectopic phospho-H3 staining was found in the maLPA$_1$-null cortex. Previous studies have shown the transcription factor Pax6 to be involved in the regulation of early neural proliferation in the developing brain (Warren and others 1999; Estivill-Torrús and others 2002) where the sequential expression of Pax6 and Tbr2 transcription factors leads the differentiation of NPCs into intermediate SVZ progenitors (Englund and others 2005; Quinn and others 2007). To see if the observed changes in the proliferative region correlated with an altered pattern of *Pax6* or *Tbr2* expression, they were analyzed by in situ hybridization and immunohistochemistry in coronal brain sections at similar embryonic ages. During early neurogenesis, dorsal telencephalic expression of *Pax6* was restricted to the VZ/SVZ where it was expressed by most NPCs (Walther and others 1991) and strongly delimited the germinative region at E14.5 (Fig. 3*C*). Examination of E14.5 maLPA$_1$-null cortex showed that the region expressing *Pax6* was noticeably reduced (Fig. 3*C*, right panel) reflecting the observed PCNA immunostaining pattern. Similarly, the region exhibiting premature expression of beta-tubulin-III, lacked *Pax6*, consistent with the loss of progenitor identity. At similar age, *Tbr2* is known to be expressed in both basal SVZ progenitors undergoing abventricular mitoses and some early postmitotic neurons delimiting the SVZ and in close association to Pax6-expressing cells underneath (Englund and others 2005; Quinn and others 2007; see Fig. 3*D*). According to a decrease of the PCNA-positive presumed VZ/SVZ of maLPA$_1$-null mice, it would be also expected a reduction in the region expressing Tbr2. Interestingly, with the slight variations, we did not found significant differences in Tbr2 expression in the maLPA$_1$-null embryonic cortex (Fig. 3*D*). Since the acquirement of intermediate progenitor SVZ cell identity is associated with upregulation of Tbr2 and downregulation of Pax6 (Englund and others 2006), our results suggest an early cell-cycle exit into the acquisition of partial SVZ identity.

In vitro proliferative behavior of NPCs isolated from wild-type and maLPA$_1$-null dissociated dorsal cortices support these differences in proliferation and maturation cellular patterning. No differences were found in survival or cell death during the experiment. BrdU labeling experiments showed fewer BrdU labeled NPCs from maLPA$_1$-null mice (Fig. 4*A,D*) accompanied by a reduction in the proportion of cells containing the

nuclear protein Cyclin A (Fig. 4*B,E*), which is selectively expressed during the S phase of the cell cycle (Darzynkiewicz and others 1996), and a correlative increase in the proportion of cells expressing $p27^{Kip1}$ (Fig. 4*C,F*), a cyclin-dependent kinase inhibitor required for VZ neural cells to exit the cell cycle and start terminal differentiation (van Lookeren-Campagne and others 1998) .

An explanation of this anomalous proliferative patterning accompanied with early expression of neuronal and differentiation markers may well be a modification in the mode of cell division. Asymmetric cell divisions correlate with neurogenesis and frequently take place with a horizontal orientation division (Chenn and McConnell 1995; Haydar and others 2003). In this sense, abventricular mitosis associated with the horizontal mode of division in SVZ (Stricker and others 2006) was not significantly increased in the maLPA$_1$-null cerebral cortex (Fig. 3*B*). To obtain a more comprehensive representation of the cortical cell division pattern, we quantified the mitotic cleavage orientations within VZ at different stages of neurogenesis. Coronal cross-sections from embryonic brains were stained with hematoxylin, which clearly identifies cells in late anaphase and telophase and facilities the observation of the cleavage plane. Sections were cut through the full rostral-caudal extent of the cortex, but no significant effect on the incidence of division was found in the different regions. The number of divisions was counted and classified by plane-of-division orientation, either vertical, horizontal or oblique, as previously described (Chenn and McConnell 1995; Estivill-Torrús and others 2002) (Supplementary Figure 3*A*). The analysis of cleavage orientations revealed a remarkable increase in the proportion of horizontal divisions in the cortex of LPA$_1$-null embryos through cortical development (Supplementary Figure 3*B*) indicating a premature conversion in the mode of cell division of LPA$_1$-null VZ as compared to wild-type.

maLPA$_1$-null mutant reveals defects in cortical formation

To characterize the function of LPA$_1$ in the developing cortex, we examined maLPA$_1$-null cortices for defects that could influence postnatal cortical organization. First, since early cytoarchitectural analysis (Fig. 1*G*)

suggested cortical layer defects in maLPA$_1$-null mice, we studied the migratory behavior of NPCs using a BrdU pulse at E14.5 to label cortical cells born at that time and examined their distribution at E18.5. The percentages of labeled cells in each location were given from the total number of exclusively labeled cells, giving an estimation of migration (Gillies and Price 1993). Immediately after the BrdU pulse, both wild-type and maLPA$_1$-null E14.5 embryos showed qualitatively similar labeling patterns with the totality of labeled cells located in the VZ/ SVZ area (data not shown). Twelve hours after BrdU administration, maLPA$_1$-null mutants showed few labeled cells in the IZ (Fig. 5*A-C*), contrasting with wild-type cortices, where most BrdU-labeled cells covered two thirds of the telencephalic wall with a significant proportion of labeled cells in the IZ. By the end of the neurogenic period (E18.5), both wild-type and maLPA$_1$-null embryos had a considerable number of E14.5-born cells (densely labeled) in the most superficial layers of the telencephalic wall (Fig. 5*D-F*), indicating that cells are capable of migration in the absence of LPA$_1$. However, further quantification of BrdU-labeled cells throughout the cortical wall demonstrated that a considerable number of both densely- and lightly-labeled cells accumulated in the deeper layers of the maLPA$_1$-null cortex (Fig. 5*E,F*), initially suggesting a positioning defect.

To determine the abnormalities in NPC migration and subsequent differentiation, additional analysis was performed. From E14.5 and during cortical development, ganglionic eminences are the major source of cortical interneurons, including parvalbumin-positive interneuron subtypes which travel to their final destination in the cortex via tangential migration (Xu and others 2004; Wonders and others 2005). A cumulative labeling of BrdU-positive cells at deeper layers could well be explained by an anomalous incorporation of neurons from tangential pathways. Immunohistochemical analysis for GAP43 – a protein expressed in early development that is involved in axonal pathfinding, neurotransmitter release and synaptic plasticity (Jacobson and others 1986) - and in situ hybridization for axonal TAG-1, expressed in developing nervous system (Yamamoto and others 1986), showed no alterations in axonal and tangential pathways when LPA$_1$ was absent (Supplementary Fig. 4*A-H*). By contrast, parvalbumin-positive neurons were reduced in the

adult maLPA$_1$-null cortex, suggesting local defects in their cortical destination rather than migration. This reduction affected particularly deep layers (Supplementary Fig. 4*I-L*) which tend normally to be enriched in parvalbumin-expressing neurons (Xu and others 2004; Wonders and others 2005).

Despite normal patterning during early stages of cortical development, the adult expression of the growth-associated protein GAP43 revealed a noticeable defect in the postnatal maLPA$_1$-null cortex. Coronal sections from P0 cortices showed GAP43 expression throughout the cortical layers in wild-type cortex (Fig. 6*A*). By contrast, maLPA$_1$-null cortices displayed less GAP43 immunoreactivity, with almost no labeling in cortical layer II (Fig. 6*B*), suggesting a defective neuronal differentiation. The neuronal identity of this GAP43-negative cortical population was confirmed with immunodetection of beta-tubulin-III (Fig. 6*C,D*). Analysis of upper cortical areas by Western blot corroborated the immunohistochemical data. Fig. 6*E* shows a typical Western blot from dissected cortical samples from wild-type and maLPA$_1$-null P0 mice stained for GAP43. Immunoreactivity mainly detected a single protein band of approximately 46 kDa. Densitometric quantitation of band intensities showed a significant (n= 8, P<0.001) reduction in GAP43 protein levels in the maLPA$_1$-null layer II cortex (Fig. 6*F*).

Taken together, these findings indicate that early embryonic maLPA$_1$-null defects in proliferation would affect normal differentiation and later cortical formation.

Increased cortical apoptosis and neuronal reduction

Previously reported receptor-mediated LPA effects on cortical folding and thickness demonstrated an anti-apoptotic role for LPA signaling (Ye and others 2002; Kingsbury and others 2003, 2004). A possible corollary of this function would be increased apoptosis following loss of LPA receptor signaling that could explain the smaller maLPA$_1$-null brain. Detection of apoptosis was performed at E15.5, after the peak in cell death in embryonic cortex, using a fluorometric apoptosis detection system based on a modified TUNEL. A more than twofold increase in the percentage of apoptotic nuclei was clearly and consistently detected in maLPA$_1$-null

cortices when compared with wild-type, predominantly at SVZ level (Fig. 7*A,D,G*). This embryonic cell death is distinct from that occurring among mature neurons associated with synaptogenesis (Blaschke and others 1998). To test whether the altered pattern of the plasticity protein GAP43 and altered differentiation correlates with later apoptotic processes, postnatal analysis was performed. Increased apoptosis was detected in maLPA$_1$-null cortex in both upper cortical areas, layers II/ III (Fig. 7*E*), and the deeper layers V/VI (Fig. 7*F*) compared with wild-type levels (Fig. 7*B,C*). Quantitative analysis revealed that the percentage of cell death was significantly higher in maLPA$_1$-null cortex, particularly in deeper cortical levels (Fig. 7*G*).

To verify whether the decrease in cerebral cortex size was due to neuronal loss, NeuN-positive neurons from primary motor cortex were counted through its rostral-caudal extension (Fig.8*A*). The numerical density of neurons (*N*v) in the primary motor cortex was determined in wild-type and maLPA$_1$ heterozygous and homozygous 12-weeks old mice using the optical dissector method (West and others 1993). Neuronal cell types were clearly identifiable with NeuN labeling (Fig. 8*B*). In coronal sections, the primary motor cortex was characterized by a prominent layer V, with a relatively low density of large pyramidal neurons, and a narrow layer IV, sparsely populated by granular neurons (Fig. 8*C,* left panel). In the absence of the LPA$_1$ receptor, the cerebral cortex was thinner than normal but cortical layers were usually similarly definable although less precise than normal (Fig. 8*C,* panel at right). The *N*v of neurons did not differ significantly among groups in layers I and IV (Table 1), although maLPA$_1$-null mice exhibited a higher density in layer I. However, the *N*v in layers II/III, V and VI was significantly lower in LPA$_1$-null motor cortex compared to wild-type, demonstrating that LPA$_1$-dependent cell reduction is markedly different at deeper cortical levels, in agreement with early neuronal defects and cell death data. In addition, post-hoc comparisons showed significant differences between heterozygous and homozygous animals in layer V and between heterozygous and wild-type in layers II/III and VI. These results indicate that LPA$_1$ is required for maintenance of normal cortical cell number.

Discussion

Our results show LPA_1-mediated signaling is important during normal embryonic cortical neurogenesis, revealed by a new LPA_1 null-mutant variant ($maLPA_1$) derived from the original (Contos and others 2000) after breeding and expansion of the colony. The absence of LPA_1 in the $maLPA_1$-null mice results in a reduction of cortical NPCs, increased apoptosis and alterations in the formation of the cerebral cortex. Earlier gain-of-function studies were essential to understand LPA receptor-mediated mechanisms, particularly in combination with mice lacking LPA_1 and LPA_2 (Kingsbury and others 2003, 2004); however, these original null-mutants have not themselves shown major cortical phenotypes (Contos and others 2000, 2002). Thus, the main finding of this study is that there is an essential *in vivo* requirement of LPA_1 during cortical development, as shown through the spontaneous generation of an LPA_1-null variant. *In vivo* observations in the developing $maLPA_1$-null cortex showed a reduced proliferative zone with premature expression of neuronal markers in the VZ/SVZ and IZ. Cortical $maLPA_1$-null NPCs isolated in culture displayed reduced proliferation and a relative overproduction of differentiated cells, supporting the changes reported previously (Kingsbury and others 2003; Rehen and others 2006) and in this study *in vivo*. These data indicate that these effects are intrinsic to the cortical cells rather than secondary indirect effects.

In the VZ, LPA released from postmitotic neurons may induce the "rounding-up" phase of interkinetic nuclear migration through cytoskeletal changes (Fukushima and others 2000, 2002; Fukushima 2004). Accordingly, an absence of LPA_1 could be expected to result in an increase in the proportion of fusiform neurons, consistent with the presence of misfated $maLPA_1$-null cells, as was observed in this study. A concomitant reduction in mitotic figures was also observed. Furthermore, LPA signaling affect the normal development of the SVZ, by virtue of the clear effects on NPCs. The proportions of symmetric nonterminal, symmetric terminal, and asymmetric cell divisions overlap during the entire developmental period (Cai and others 2002; Noctor and others 2004). Our studies here presented describe an increase in the proportions of apical NPCs exhibiting horizontal cleavage plane in absence of LPA_1 receptor. Even though the orientation of the cleavage

plane is an insufficient criterion to predict the mode of division, oblique and horizontal cleavage plane are still the most likely to produce asymmetric divisions by generating unequal separation of apical components (Haydar and others 2003; Götz M and Huttner WB 2005; Buchman and Tsai 2007). It has been recently demonstrated that LPA–induced enhancement of neuronal differentiation via LPA_1 is mediated by its interaction with G protein subunit Gi/o (Fukushima and others 2007). Interestingly, overexpression of Gi subunit has been suggested to result in mitotic spindle destabilization (Du and Macara 2004). Last studies on VZ/SVZ division have called attention to intermediate SVZ progenitors which division mostly generates two neurons in symmetrical way in neurogenic phase (Haydar and others 2003; Haubensak and others 2004; Miyata and others 2004; Noctor and others 2004; Götz M and Huttner WB 2005; Kriegstein and others 2006). In view of that, the observed preponderance of horizontal cleavages in maLPA_1-null apical NPCs would correlate with a subsequent increase of intermediate SVZ progenitors undergoing mitosis. However, and quite opposite, abventricular division is not significantly increased in favour of early maturation and apoptosis. In this sense, we should consider as a possible explanation the apparent changes in cell polarity and restructuring of apical /basal processes (as seen by the increase in horizontally oriented fusiform cells) because of their relevance in the government of cell division and fate determination (Miyata and others 2004; Götz M and Huttner WB 2005; Cappello and others 2006; Buchman and Tsai 2007). Thus, LPA_1-induced deficient proliferation and morphological changes, not mutually exclusive, would lead to an anomalous incomplete asymmetry which produces mispositioned premature VZ and SVZ cells and early apoptosis as immediate consequences.

Programmed cell death plays an important role in cortical development (Blaschke and others 1996, 1998), and the increased apoptosis in maLPA_1-null embryos agrees with the proposed role for LPA in neuronal survival and normal cortical formation (Kingsbury and others 2003, 2004; Ye and others 2002). From our results the effect of LPA_1 absence would result as a cooperative summation of altered proliferation and apoptosis. While in vitro and in vivo observations have showed consistency respecting the effect of LPA absence on

survival/apoptosis, its consequences in proliferation continues under some discrepancies since LPA have been demonstrated to increases the number of mitotic cells without increasing proliferation by itself (Kingsbury and others 2003, 2004). Significantly maLPA$_1$-null mice exhibit a decrease of the number of mitoses in both ventricular and abventricular location. However it seems difficult to determinate how this reduction may influence directly the final apoptosis rate rather than be this a secondary effect attributable to an early postmitotic state, especially considering that neuroproliferative apoptosis does not become evident until differentiating postmitotic cells are present (Blaschke and others 1998).

As above mentioned SVZ cells play an important role in the maintenance of cortical expansion and novel regulators are now being known to influence the fate of apical VZ NPCs into SVZ, acquiring division and fate determinants of SVZ progenitors (Cappello and others 2006). LPA would suitably be included among these since it has been proposed to be released by postmitotic neurons and influence the nuclear organization, morphology and normal migration of VZ NPCs (Fukushima and others 2000, 2002). Both, in vitro LPA addition and LPA$_1$ absence generate a direct effect onto subsequent SVZ organization and maturation. However, whereas LPA produces in vitro a displacement of mitotic cells into SVZ (Kingsbury and others 2003, 2004; Rehen and others 2006) and morphological changes in cell processes (Fukushima and others 2000, 2002; Rehen and others 2006) not in discrepancy with a concomitant postmitotic LPA release on demand of NPCs ratio (Fukushima and others 2000), the deletion of LPA$_1$-signaling pathway in maLPA$_1$-null mice would result in the real blockage of this postmitotic control on VZ NPCs generating a failure of cell cycle and a reduction in proliferation with the subsequent cited effects.

During normal embryonic development, differences in NPC proliferation may underlie the variations in laminar thickness in the cerebral cortex (Caviness and others 1995; Rakic 1995). Both cell-intrinsic and -extrinsic factors contribute to changes in cell production affecting cortical growth and neuron survival. The genetic and molecular mechanisms underlying these processes are not completely understood. Recently, it has been demonstrated that extrinsic cues in the VZ environment of NPCs are able to restrict their fate (Campbell

2005). The NPC alterations described here in the maLPA$_1$-null mice provide evidence for the *in vivo* participation of LPA$_1$ signaling in these neurogenic processes, particularly those concerning maturing and apoptosis.

In addition to abnormal proliferation and survival, many maLPA$_1$-null forebrain neurons appear to arrest in the deeper cortical layers rather than migrating to more superficial sites, consistent with the initial abnormal positioning of mutant cells and increased postnatal apoptosis in layers V/VI. Whereas *lpa*$_1$ is enriched in the VZ, *lpa*$_2$ is enriched in the embryonic postmitotic regions at the end of neurogenesis (Hecht and others 1996; Contos and others 2001). Later in development, partial compensation by LPA$_2$ (Contos and others 2001) may rescue some of these mispositioned neurons postnatally, giving rise to the abnormal but discernible conventionally layered cortex seen in the maLPA$_1$-null, although this remains to be determined experimentally. Conversely, analysis of axonal and tangential cortical pathways as well as parvalbumin-positive cell location suggested intriguing local defects in their destination rather than migration. Further analysis would be necessary to discriminate precisely a failure in cells to reach their destination from an impaired normal differentiation, or the occurrence of both combined defects.

The reduced perinatal expression of GAP43 in the maLPA$_1$-null cortex suggests LPA$_1$-dependent sequels linked to the function of GAP43, such as synapse formation and neural plasticity and the development of normal serotoninergic innervation in the cortex (Donovan and others 2001); thus, anomalous synaptic connectivity could well result in both wiring defects and increased apoptosis. Further insights into the consequences of these cortical defects on brain function are necessary.

The new maLPA$_1$-null variant demonstrates a role for LPA$_1$ in normal cortical development and for maintaining normal cohorts of NPCs that was not seen in the original null mutant. The cortical abnormalities of the maLPA$_1$-null variant support the existence of unidentified, brain-specific LPA-signaling genetic modifier(s), in view of the otherwise shared phenotype of maLPA$_1$-null and the original LPA$_1$-null mutants.

The reason for the modified phenotype of the original LPA_1-null mice that appeared in Málaga is not known. This, i.e., the presence of unknown modifiers on a single mutant allele, is common fact in studies addressing the spontaneous variance of mutant phenotypes. Variant mutant phenotypes are not uncommon, as documented by major influences of background strain (Sibilia and Wagner 1995). Well known examples that affect the brain include caspase deficient animals as well as the *Orl* allele of Reeler (Goffinet 1990; Nadeau 2001; Rice and Curran 2001; Leonard and others 2002; Bergren and others 2005). In both of these cases, and the vast majority of reported strain-dependent differences, the full range of modifiers is not known. Genetic modifiers such as other genes, viruses, retrotransposons, etc., may contribute to the new phenotype, and identifyinfg them exceed the aims of the present studies. However, because maLPA$_1$-null mice have allowed the establishment of a highly penetrant and reproducible phenotype, this should serve as a starting point towards understanding and identifying interacting genes or non-gene elements in future studies.

These findings may have relevance to developmental disorders of the CNS, such as dysregulation of apoptosis, microcephaly and mental health (Haydar and others 2000; Kadota and others 2002; Bérubé and others 2005). These data also add to a growing number of lysophospholipid-dependent functions that impact on normal organism development and function. It will thus be of interest to compare the more pronounced phenotype of maLPA$_1$-null mice to the phenotypic defects related to psychiatric diseases observed in non-variant mutants (Harrison and others 2003).

Supplementary Material

Supplementary material can be found at: http://www.cercor.oxfordjournals.org/.

Notes

We are indebted to F.J. Tejedor at Instituto de Neurociencias (CSIC-UMH, Alicante) for useful discussion regarding this work; J.A. Aguirre, from Dept. of Physiology at University of Málaga, for accessibility with stereology; animal housing facilities of University of Málaga for maintenance of mice and technical

assistance, Elvira Gil Lara for technical support, Christine Paczkowski for reading the manucript and Ian Johnstone for help with language corrections. Our work received grants from the Human Frontier Science Programme, (JC, FRDF), FIS 01/3032 (GE), FIS 02/1643 (GE), FIS 02/1517 (PF) and Red CIEN (G03/06) (FRDF) (Instituto de Salud Carlos III, Ministerio de Sanidad) and the National Institutes of Health (USA) MH51699 and MH01723 (JC).

Address correspondence to Guillermo Estivill-Torrús, Unidad de Investigación, Fundación IMABIS, Hospital Carlos Haya, Pabellón A, planta 7ª, Avenida Carlos Haya 82, E-29010 Málaga, Spain. Email: guillermo.estivill@fundacionimabis.org.

References

Anliker B, Chun J. 2004. Lysophospholipid G protein-coupled receptors. J Biol Chem 279: 20555-20558.

Bayer SA, Altman J. 1991. Neocortical development. New York: Raven Press.

Bergren SK, Chen S, Galecki A, Kearney JA. 2005. Genetic modifiers affecting severity of epilepsy caused by mutation of sodium channel Scn2a. Mamm Genome 16:683-690.

Bérubé NG, Mangelsdorf M, Jagla M, Vanderluit J, Garrick D, Gibbons RJ, Higgs DR, Slack RS, Picketts DJ. 2005. The chromatin-remodeling protein ATRX is critical for neuronal survival during corticogenesis. J Clin Invest 115:258–267.

Blaschke AJ, Staley K, Chun J.1996. Widespread programmed cell death in proliferative and postmitotic regions of the fetal cerebral cortex. Development 122: 1165-1174.

Blaschke AJ, Weiner JA, Chun J. 1998. Programmed cell death is a universal feature of embryonic and postnatal neuroproliferative regions throughout the central nervous system. J Comp Neurol 396: 39-50.

Buchman JJ, Tsai L. 2007. Spindle regulation in neural precursors of flies and mammals. Nat Rev Neurosci 8: 89-100.

Cai L, Hayes NK, Takahashi T, Caviness VSJr, Nowakowski RS. 2002. Size distribution of retrovirally marked lineages matches prediction from population measurements of cell cycle behaviour. J Neurosci Res 69: 731-744.

Campbell K. 2005. Cortical neuron specification: it has its time and place. Neuron 46: 373–376.

Caviness VSJr, Takahashi T, Nowakowsky RS. 1995. Numbers, time and neocortical neurogenesis: a general developmental and evolutionary model. Trends Neurosci 18: 379-383.

Chenn A, McConnell SK. 1995. Cleavage orientation and the asymmetric inheritance of Notch 1 immunoreactivity in mammalian neurogenesis. Cell 82: 631-641.

Chun J, Goetzl EJ, Hla T, Igarashi Y, Lynch KR, Moolenaar W, Pyne S, Tigyi G. 2002. International union of pharmacology. XXXIV. Lysophospholipid receptor nomenclature. Pharmacol Rev 54: 265–269.

Chun J. 2005. Lysophospholipids in the nervous system. Prostaglandins Other Lipid Mediat 77: 46-51.

Contos JJA, Chun J. 2001. The mouse lpA3/Edg7 lysophosphatidic acid receptor gene: genomic structure, chromosomal localization, and expression pattern. Gene 267: 243–253.

Contos JJA, Ishii I, Fukushima N, Kingsbury MA, Ye X, Kawamura S, Brown JH, Chun J. 2002. Characterization of lpa2 (Edg4) and lpa1/lpa2 (Edg2/Edg4) lysophosphatidic acid receptor knockout mice: signaling deficits without obvious phenotypic abnormality attributable to lpa2. Mol Cell Biol 22: 6921–6929.

Contos JJA, Fukushima N, Weiner JA, Kaushal D, Chun J. 2000. Requirement for the lpa_1 lysophosphatidic acid receptor gene in normal suckling behavior. Proc Natl Acad Sci 97: 13384- 13389.

Darzynkiewicz Z, Gong J, Juan G, Ardelt B, Traganos F. 1996. Cytometry of cyclin proteins. Cytometry 25: 1-13.

Dash PK, Orsi SA, Moody M, Moore AN. 2004. A role for hippocampal Rho–ROCK pathway in long-term spatial memory. Biochem Biophys Res Commun 322: 893-898.

Denaxa M, Chan CH, Schachner M, Parnavelas JG and Karagogeos D. 2001. The adhesion molecule TAG-1 mediates the migration of cortical interneurons from the ganglionic eminence along the corticofugal fiber system. Development 128: 4635-4644.

Donovan SL, Mamounas LA, Andrews AM, Blue ME, McCasland JS. 2002. GAP-43 is critical for normal development of the serotonergic innervation in forebrain. J Neurosci 22: 3543–3552.

Du Q, Macara IG. 2004. Mammalian Pins is a conformational switch that links NuMA to heterotrimeric G proteins. Cell 119: 503–516.

Dubin AE, Bahnson T, Weiner JA, Fukushima N, Chun J. 1999. Lysophosphatidic acid stimulates neurotransmitter-like conductance changes that precede GABA and L-glutamate in early, presumptive cortical neuroblasts. J Neurosci 19: 1371–1381.

Englund C, Fink A, Lau C, Pham D, Daza RAM, Bulfone A, Kowalczyk T, Hevner RF. 2005. Pax6, Tbr2, and Tbr1 are expressed sequentially by radial glia, intermediate progenitor cells, and postmitotic neurons in developing neocortex. J Neurosci 25:247–251.

Estivill-Torrús G, Pearson H, van Heyningen V, Price DJ, Rashbass P. 2002. Pax6 is required to regulate the cell cycle and the rate of progression from symmetrical to asymmetrical division in mammalian cortical progenitors. Development 129: 455-466.

Fujiwara Y, Sebok A, Meakin S, Kobayashi T, Murakami-Murofushi K, Tigyi G. 2003. Cyclic phosphatidic acid elicits neurotrophin-like actions in embryonic hippocampal neurons. J Neurochem 87: 1272–1283.

Fukushima N. 2004. LPA in neural cell development. J Cell Biochem 92: 993-1003.

Fukushima N, Weiner JA, Chun J. 2000. Lysophosphatidic acid (LPA) is a novel extracellular regulator of cortical neuroblast morphology. Dev Biol 228: 6-18.

Fukushima N, Weiner JA, Kaushal J, Contos JJA, Rehen SK, Kingsbury MA, Kim KY, Chun J. 2002. Lysophosphatidic acid influences the morphology and motility of young, postmitotic cortical neurons. Mol Cell Neurosci 20: 271-282.

Fukushima N, Shano S, Moriyama R, Chun J. 2007. Lysophosphatidic acid stimulates neuronal differentiation of cortical neuroblasts through the LPA1–Gi/o pathway. Neurochem Int 50: 302-307.

Gardell SE, Dubin AE, Chun J. 2006. Emerging medicinal roles for lysophospholipid signaling. Trends Mol Med 12: 65-75.

Gillies K, Price DJ. 1993. The fates of cells in the developing cerebral cortex of normal and methylazoxymethanol acetate-lesioned mice. Eur J Neurosci 5: 73-84.

Goffinet AM. 1990. Cerebellar phenotype of two alleles of the 'reeler' mutation on similar backgrounds. Brain Res 519: 355-357.

Harrison SM, Reavill C, Brown G, Brown JT, Cluderay JE, Crook B, Davies CH, Dawson LA, Grau E, Heidbreder C, Hemmati P, Hervieu G, Howarth A, Hughes ZA, Hunter AJ, Latcham J, Pickering S, Pugh P, Rogers DC, Shilliam CS, Maycox PR. 2003. LPA1 receptor-deficient mice have phenotypic changes observed in psychiatric disease. Mol Cell Neurosci 24: 1170- 1179.

Haubensak W, Attardo A, Denk W, Huttner WB. 2004. Neurons arise in the basal neuroepithelium of the early mammalian telencephalon: A major site of neurogenesis. Proc Natl Acad Sci 101: 3196-3201.

Haydar TF, Nowakowski RS, Yarowsky PJ, Krueger BK. 2000. Role of founder cell deficit and delayed neuronogenesis in microencephaly of the trisomy 16 mouse. J Neurosci 20: 4156–4164.

Haydar TF, Ang EJr, Rakic P. 2003. Mitotic spindle rotation and mode of cell division in the developing telencephalon. Proc Natl Acad Sci 100: 2890- 2895.

Hecht JH, Weiner JA, Post SR, Chun J. 1996. Ventricular zone gene-1 (vzg-1) encodes a lysophosphatidic acid receptor expressed in neurogenic regions of the developing cerebral cortex. J Cell Biol 135: 1071–1083.

Hendzel MJ, Wei Y, Mancini MA, van Hooser A, Ranalli T, Brinkley BR, Bazett-Jones DP, Allis CD. 1997. Mitosis-specific phosphorylation of histone H3 initiates primarily within pericentromeric heterochromatin during G2 and spreads in an ordered fashion coincident with mitotic chromosome condensation. Chromosoma 106: 348–360.

Ino H, Chiba T. 2000. Expression of proliferating cell nuclear antigen (PCNA) in the adult and developing mouse nervous system. Brain Res Mol Brain Res 78: 163-174.

Ishii I, Fukushima N, Ye X, Chun J. 2004. Lysophospholipid receptors: signaling and biology. Ann Rev Biochem 73: 321-354.

Jacobson RD, Virag I, Skene JH. 1986. A protein associated with axon growth, GAP-43, is widely distributed and developmentally regulated in rat CNS. J Neurosci 6: 1843–1855.

Jin K, Zhu Y, Sun Y, Mao XO, Xie L, Greenberg DA. 2002. Vascular endothelial growth factor (VEGF) stimulates neurogenesis in vitro and in vivo. Proc Natl Acad Sci 99: 11946–11950.

Kadota M, Shirayoshi Y, Oshimura M. 2002. Elevated apoptosis in pre-mature neurons differentiated from mouse ES cells containing a single human chromosome 21. Biochem Biophys Res Commun 299:599–605.

Kingsbury MA, Rehen SK, Contos JJA, Higgins CM, Chun J. 2003. Non-proliferative effects of lysophosphatidic acid enhance cortical growth and folding. Nat Neurosci 6: 1292–1299.

Kingsbury MA, Rehen SK, Ye X, Chun J. 2004. Genetics and cell biology of lysophosphatidic acid receptor-mediated signaling during cortical neurogenesis. J Cell Biochem 92: 1004-1012.

Kriegstein A, Noctor S, Martínez-Cerdeño V. 2006.Patterns of neural stem and progenitor cell division may underlie evolutionary cortical expansion. Nat Rev Neurosci 7: 883-890.

Lee CW, Rivera R, Gardell S, Dubin AE, Chun J. 2006. GPR92 as a new G12/13 and Gq coupled lysophosphatidic acid receptor that increases cAMP: LPA5. J Biol Chem (in press; doi: 107410./jbc.M603670200).

Leonard JR, Klocke BJ, D'Sa C, Flavell RA, Roth KA. 2002. Strain-dependent neurodevelopmental abnormalities in caspase-3-deficient mice. J Neuropathol Exp Neurol 61:673-677.

Lu WY, Xiong ZG, Lei S, Orser BA, Dudek E, Browning MD, MacDonald JF. 1999. G-protein-coupled receptors act via protein kinase C and Src to regulate NMDA receptors. Nat Neurosci 2: 331–338 .

Menezes JR, Luskin MB. 1994. Expression of neuron-specific tubulin defines a novel population in the proliferative layers of the developing telencephalon. J Neurosci 14: 5399–5416.

Miyata T, Kawaguchi A, Saito K, Kawano M, Muto T, Ogawa M. 2004. Asymmetric production of surface-dividing and non-surface-dividing cortical progenitor cells. Development 131: 3133-3145.

Nadeau JH. 2002. Modifier genes in mice and humans. Nat Rev Gen 2:165-174.

Noctor SC, Martínez-Cerdeño V, Ivic L. Kriegstein A. 2004.Cortical neurons arise in symmetric and asymmetric division zones and migrate through specific phases. Nat Neurosci 7:136-144

Qian X, Davis AA, Goderie SK, Temple S. 1997. FGF2 concentration regulates the generation of neurons and glia from multipotent cortical stem cells. Neuron 18: 81–93.

Quinn JC, Molinek M, Martynoga BS, Zaki PA, Faedo A, Bulfone A, Hevner RF, West JD, Price DJ. 2007. Pax6 controls cerebral cortical cell number by regulating exit from the cell cycle and specifies cortical cell identity by a cell autonomous mechanism. Dev Biol 302: 50-65.

Rakic P. 1995. A small step for the cell, a giant leap for mankind: a hypothesis of neocortical expansion during evolution. Trends Neurosci 18: 383-388.

Rehen SK, Kingsbury MA, Almeida BSV, Herr DR, Peterson S, Chun J. 2006. A new method of embryonic culture for assessing global changes in brain organization. J Neurosci Meth (in press; doi: 10.1016/j.jneumeth.2006.05.025).

Reynolds BA, Tetzlaff W, Weiss S. 1992. A multipotent EGF-responsive striatal embyronic progenitor cell produces neurons and astrocytes. J Neurosci 12: 4565–4574.

Rice DS, Curran T. 2001. Role of the reelin signaling pathway in central nervous system development. Ann Rev Neurosci 24:1005-1039.

Sibilia M, Wagner EF. 1995. Strain-dependent epithelial defects in mice lacking the EGF receptor. Science 269: 234–238.

Sidman RL, Miale IL, Feder N. 1959. Cell proliferation and migration in the primitive ependymal zone: an autoradiographic study of histogenesis in the nervous system. Exp Neurol 1: 322-333.

Stricker SH, Meiri K, Götz M. 2006. P-GAP-43 is enriched in horizontal cell divisions throughout rat cortical development. Cerebral Cortex (in press; doi:10.1093/cercor/bhj171)

Takahashi T, Goto T, Miyama S, Nowakowski RS, Caviness VSJr. 1999. Sequence of neuron origin and neocortical laminar fate: relation to cell cycle of origin in the developing murine cerebral wall. J Neurosci 19: 10357-10371.

Van Lookeren-Campagne M, Gill R. 1998. Tumor-suppressor p53 is expressed in proliferating and newly formed neurons of the embryonic and postnatal rat brain: comparison with expression of the cell cycle regulators p21waf1, p27Kip1, p57Kip2, p16Ink4a, cyclin G1, and the protooncogene Bax. J Comp Neurol 397: 181–198.

Walther C, Gruss P. 1991. Pax-6, a murine paired box gene, is expressed in the developing CNS. Development 113: 1435–1449.

Warren N, Caric D, Pratt T, Clausen JA, Asavaritikrai P, Mason JO, Hill RE, Price DJ. 1999. The transcription factor, Pax6, is required for cell proliferation and differentiation in the developing cerebral cortex. Cereb Cortex 9: 627-635.

West MJ. 1993. New stereological methods for counting neurons. Neurobiol Aging 14: 275–285.

Wonders C and Anderson SA. 2005. Cortical interneurons and their origins. The Neuroscientist 11: 199-205.

Xu Q, Cobos I, De La Cruz E, Rubenstein JLR, Anderson SA. 2004. Origins of cortical interneuron subtypes. J Neurosci 24:2612–2622.

Yamamoto M, Boyer AM, Crandall JE, Edwards M and Tanaka H. 1986. Distribution of stage-specific neurite-associated proteins in the developing murine nervous system recognized by a monoclonal antibody. J Neurosci 6: 3576-3594.

Ye X, Ishii I, Kingsbury MA, Chun J. 2002. Lysophosphatidic acid as a novel cell survival/ apoptotic factor. Biochim Biophys Acta 1585: 108–113.

Table 1

Neuronal quantification in control and maLPA$_1$ null mice

motor cortex			
genotype	ma*lpa*$_1$ **+ / +**	ma*lpa*$_1$ **+ / -**	ma*lpa*$_1$ **- / -**
Layer I	30.9 ± 2.21	24.6 ± 17.7	43.7 ± 7.44
Layer II/III	250 ± 30.4	172 ± 8.02*	164 ± 17.4 **
Layer IV	215 ± 6.16	185 ± 18.6	179 ± 9.75
Layer V	148 ± 3.79	136 ± 9.58	113 ± 7.97 ** #
Layer VI	228 ± 7.65	184 ± 2.28 *	159 ± 9.43 **

Estimation of the numerical density of neurons (N_V, neurons/mm3; expressed as the mean ± SEM) in individual layers of the primary motor regions of the cerebral cortex for wild type (ma$lpa_1^{(+/+)}$), heterozygous (ma$lpa_1^{(+/-)}$), and homozygous (ma$lpa_1^{(-/-)}$), 12-week old mice. n = 6, *, P<0.05 and **, P<0.005 as compared with wild-type group; #, P<0.05 as compared with heterozygous group.

Captions

Figure 1.

Gross anatomy and cerebral morphological defects in maLPA$_1$-null mice

(***A***) Three-month-old homozygous ma*lpa*$_1^{(-/-)}$ mice are smaller in size and exhibit craniofacial deformities and shortened snouts when compared with wild-type ma*lpa*$_1^{(+/+)}$ littermates. Note the spherical and reduced aspect of the mutant head. (***B***) Total body mass estimations (according to Contos and others 2004) for male (left) and female (right) ma*lpa*$_1^{(-/-)}$ mice (●) and ma*lpa*$_1^{(+/-)}$ littermates (○) from ma*lpa*$_1^{(+/-)}$ x ma*lpa*$_1^{(+/-)}$ matings. Data are expressed as means ± SD (n=14). *, P, 0.05 (repeated measures were analyzed with ANOVA). Mass data for ma*lpa*$_1^{(+/+)}$ littermates that overlapped those shown for ma*lpa*$_1^{(+/-)}$ are not presented for clarity. (***C***) Dorsal and side views of three-month-old wild-type, ma*lpa*$_1^{(+/+)}$ and ma*lpa*$_1^{(-/-)}$ brains, showing that deleting *lpa*$_1$ results in a rounding and reduction of telencephalic vesicles and olfactory bulb (arrowhead). (***D***) Brain wet weight (means ± s.e.m; n=14) at cited age for male ma*lpa*$_1^{(-/-)}$ mice, ma*lpa*$_1^{(+/-)}$ and control ma*lpa*$_1^{(+/+)}$ littermates. *, P, 0.05 (analyzed with ANOVA). Significant differences were detected between maLPA$_1$-null brain and their wild-type and heterozygous counterparts. (***E***) Hematoxylin-eosin stained sagittal sections of E18.5 wild-type and maLPA$_1$-null littermates showing similar gross anatomy. (***F***) Histological coronal brain sections stained with hematoxylin showing the reduction in size and cortical thickness of the maLPA$_1$-null brain (right panel) when compared with wild-type control (at left) at E18.5. (***G***) Sections showing normal cortical thickness and six-layered cortex from P0 wild-type mice and equivalent for maLPA$_1$-null brain. Cortical layers, as deduced from cell size and packing density, are indicated by Roman numerals I through VI. Undersized telencephalic wall from maLPA$_1$-null mice exhibits a reduced layer I and there is no clear layering at deeper levels. Arrow (***G***, right) indicates cortical surface disruption. Scale bars in (*F*) represent 600 µm whereas in (*G*) they represent 100 µm.

Figure 2.

Cortical proliferative patterning is affected in mice lacking LPA_1.

Expression patterns of PCNA and beta-tubulin-III in E11.5 sagittal (***A-L***) and E14.5 coronal (***M-X***) sections from the cerebral cortex of wild-type (***A, B, G, J, M, N, S, V***), ma*lpa*$_1$ heterozygous (***C, D, H, K, O, P, T, W***) and ma*lpa*$_1$-null (***E, F, I, L, Q, R, U, X***) embryos. Images are false color-converted from originally obtained. By E11.5 the absence of *lpa*$_1$ resulted in a slight reduction of PCNA immunoreactive area (***I***) and early expression of beta-tubulin-III in VZ cells (arrows in ***K*** an ***L***), predominantly next to the ventricular surface. At E14.5, an anomalous germinative layering resulted when the receptor was absent in comparison with wild-type patterning, demonstrated by a reduction of PCNA in VZ/ SVZ and a premature strong expression of beta-tubulin-III in that area (arrows in ***W*** and ***X***). At this age beta-tubulin-III immunodetection showed a disturbance in cortical radial organization with fibers running parallel to ventricular surface (arrowheads in ***W*** and ***X***). Broken lines delimit marker expression. Depicted squares (*A-F, M-R*) are magnified 10x in the next images. CP, cortical plate; PP, preplate ; VZ, ventricular zone; VZ/SVZ, ventricular plus subventricular zones. Scale bars in (A-F), 250 μm; (*G-L*), 55 μm; (*M-R*), 300 μm; (*S-X*), 65 μm.

Figure 3.

Absence of LPA_1 signaling alters the proportion of mitosis and Pax6 expression area.

(***A***) Mitotic figures detected in E14.5 cortical coronal VZ by immunolabeling with anti phospho-H3 for wild type (wt) and maLPA$_1$-null (null) mice. (***B***) Histogram depicts further analysis of cross sections showing the percentage of phospho-H3 stained cells from the total and the significant decrease in the proportion of mitosis observed for heterozygous and homozygous maLPA$_1$-null embryos (t-test, n= 8; **, P=0.01). Plots represent VZ and SVZ (abventricular) percentages. (***C, D***) Coronal brain sections (normal and magnified squares) from E14.5 wild-type and homozygous mutant littermates processed for in situ hybridization for *Pax6* expression (***C***) and Tbr2 immunostaining (***D***). The loss of LPA_1 generates a VZ/ SVZ showing reduction of *Pax6* expression and exhibiting remarkable levels of Tbr2 expression (***D***). Scale bars in (*A*), 45 μm; (*C, D*) 400 μm.

Figure 4

In vitro analysis of maLPA$_1$-null cortical precursors.

(***A***) Histograms representing the percentages of BrdU-positive cells from the total after a 45 minute pulse given 12 hours after plating. Significant reduction in BrdU incorporation (P<0.05; ANOVA tested) was observed between cultures of wild-type and maLPA$_1$-null cells at all time-points. *, significance vs. wild-type control; **, significance between null homozygous and heterozygous NPC cultures. (***B, C***) Percentages of cells expressing Cyclin A (***B***) and p27^{kip1} (***C***) throughout culture period. Wild-type cells showed no significant changes in the number of cells expressing Cyclin A and a small increase in p27^{kip1} expression over the culture period. By contrast, maLPA$_1$-null NPCs display a significant (P<0.05) decrease in the percentage of cells expressing Cyclin A and a substantial increase in p27^{kip1} expressing cells 24 hours after plating. (***D-F***) Immunocytochemically detected differences in BrdU labeling. (***D***), Cyclin A expression (***E***) and p27^{kip1} (***F***) in wild-type (left panel) and maLPA$_1$-null (right panel) NPC cultures 18 hours after plating. Specific staining is detected as brown label with beta-tubulin-III counterstaining (blue label). Scale bars in (*A*), 20 µm and (*G-I),* 25µm.

Figure 5

Cortical cells accumulate at deeper CP layers in maLPA$_1$-null mice.

Contribution of neural precursor migration in cortical layering was analyzed by examining the patterns of BrdU labeling in the E18.5 cortex (middle position) after embryos were BrdU injected on E14.5. Data were analyzed at 12h after injection (***A-C***) and by E18.5 (***D-F***). (***A,D***) Coronal cortical sections of E14.5 (***A***) and E18.5 (***D***) wild type (wt) and maLPA$_1$-null (null) embryos immunostained for BrdU. E18.5 sections were counted in 100 μm width radial strips further subdivided by depth, comprising the cortical plate (CP) and intermediate zone (IZ). Boundaries between layers are indicated by broken lines; (MZ), marginal zone. (***B,F***) Percentages of dense (***B,E***) and light (***C,F***) labeled cells in each cortical bin (75 x 100 μm) are represented against depth. Graphs show the average densities (± s.e.m) of BrdU-labeled cells. In contrast with the wild-type pattern, the proportion from both densely and lightly labeled cells in maLPA$_1$-null cortex (null) is dramatically reduced in the IZ 12h after the single BrdU pulse. By E18.5, maLPA$_1$-null mice show a significant increase in BrdU-labeled cells (n=8; **, P<0.001) in those bins corresponding to deeper levels of the cortical area immediately past the IZ, as compared with wild-type pattern. Abbreviations as previously mentioned. Scale bar in (*A,D*), 100 μm.

Figure 6

Cortical maldevelopment in maLPA$_1$-null mice results in GAP43 deficiency.

(***A,B***) Coronal sections of P0 wild-type (***A***) and maLPA$_1$-null (***B***) cortex immunostained for GAP43. The insert is magnified 3x from each section and illustrates the reduction in immunoreactivity in maLPA$_1$-null superficial layers relative to wild-type. (***C,D***) Beta-tubulin-III immunostaining at corresponding levels in A and B. Cortical layering is indicated by Roman numerals. Scale bar in (*A,B*), 300 μm; (*C,D*), 175 μm. (***E***) A representative Western-blot of GAP43 in P0 wild-type and maLPA$_1$ null cortical areas depicted as above, showing the reduced immunostaining for maLPA$_1$-null samples, specially in area 1 corresponding to the upper medial-dorsal portion of cortical layer II. (***F***) Densitometric analysis of band intensities confirmed the reduced

expression in the absence of LPA_1, almost absent in area 1 (t-test, *n*=8, as separated experiments; **, wt1 vs. null1, P<0.001; * wt2 vs. null2, P<0.001).

Figure 7

Cortical apoptosis is increased in maLPA$_1$-null mice.

(***A-F***) Representative photographs of E15.5 (***A,D***) and P7 (***B,C,E,F***) cortical coronal sections from wild-type (wt, ***A-C***) and maLPA$_1$-null (null, ***D-F***) mice showing labeled nuclei with DeadEnd™ Colorimetric Apoptosis Detection System in E15.5 cortices (***A,D***) and P7 cortical layers II/III (***B,E***) and VI (***C,F***) at the dorsal-medial level of the cortex. (***G***) Graph shows the quantified percentage of labeled nuclei for mentioned cortical areas. Although significant differences between genotypes are observed for both cortical areas, note the remarkable increase in the proportion of apoptotic nuclei at developmental age E15.5 and in postnatal deeper cortical regions (*, P<0.005 for comparison wt vs. null for layer II/III, P<0.001 when tested in E15.5 cortex and cortical layer VI, t-test, *n*=8). Scale bars, 150 µm (*A,D*) and 110 µm (*B,C,E,F*).

Figure 8

Stereological analysis of cerebral cortex for neuronal quantification in maLPA$_1$ null mice.

(***A,B***) Representative sections (30 µm thick) of immunostaining against the neuron-specific protein NeuN throughout the cerebral hemispheres of homozygous maLPA$_1$-null adult littermates. Sections illustrate the rostral (***A,*** left image) and more caudal (***A,*** at right) sections through the primary motor cortex in the maLPA$_1$-null mice wherein the lamination is still definable to demarcate the layers. Predicted Bregma is given. Similar sections were considered in wild-type and heterozygous mice. Boxes show the measured regions. (***B***) Representative image of layer V from the previous picture. White arrowheads show neurons positive for NeuN immunolabeling. (***C***) Photomicrographs of the primary motor cortex (NeuN immunostained) showing the pattern of usual cortical lamination in the wild-type and maLPA$_1$-null mice. Cortical layers indicated by Roman numerals I through VI. Scale bars in (*A,B*), 1mm; (*C*), 200 µm; (*D*), 25 µm.

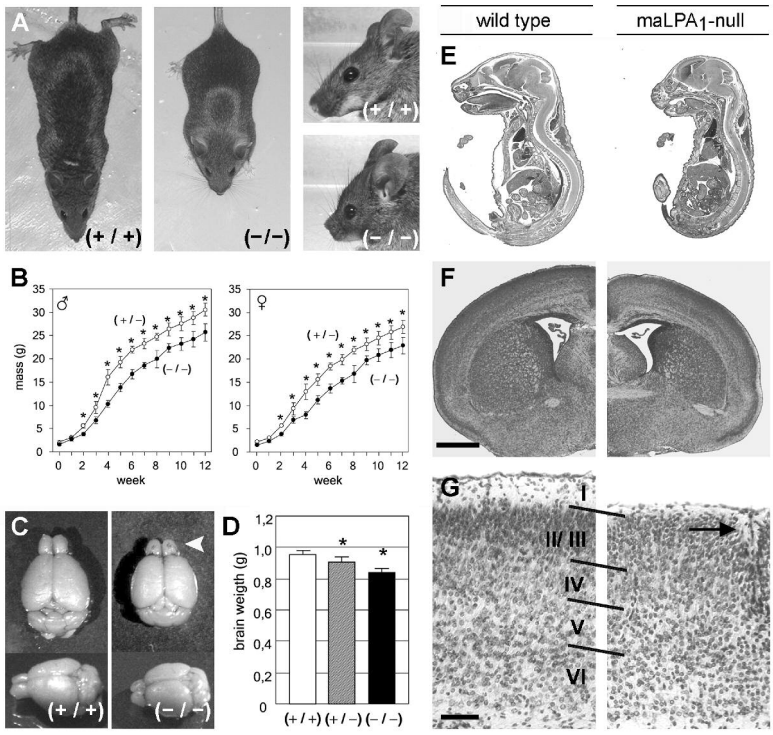
A
(+ / +)
(−/−)
(+ / +)
(− / −)
wild type
maLPA1-null
E
B
♂
♀
mass (g)
week
(+/−)
(− / −)
F
G
I
II/ III
IV
V
VI
C
D
brain weigth (g)
(+ / +) (+ / −) (− / −)

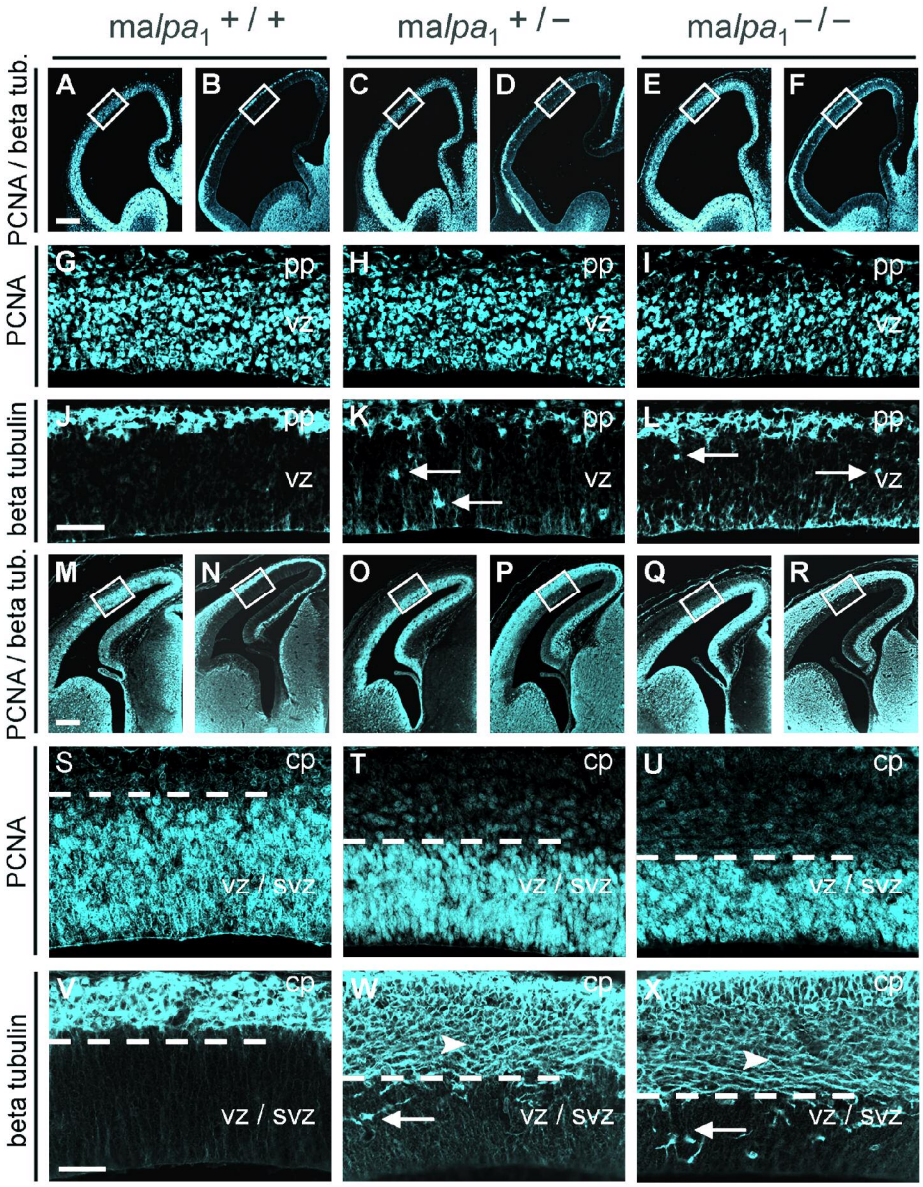

140x179mm (300 x 300 DPI)

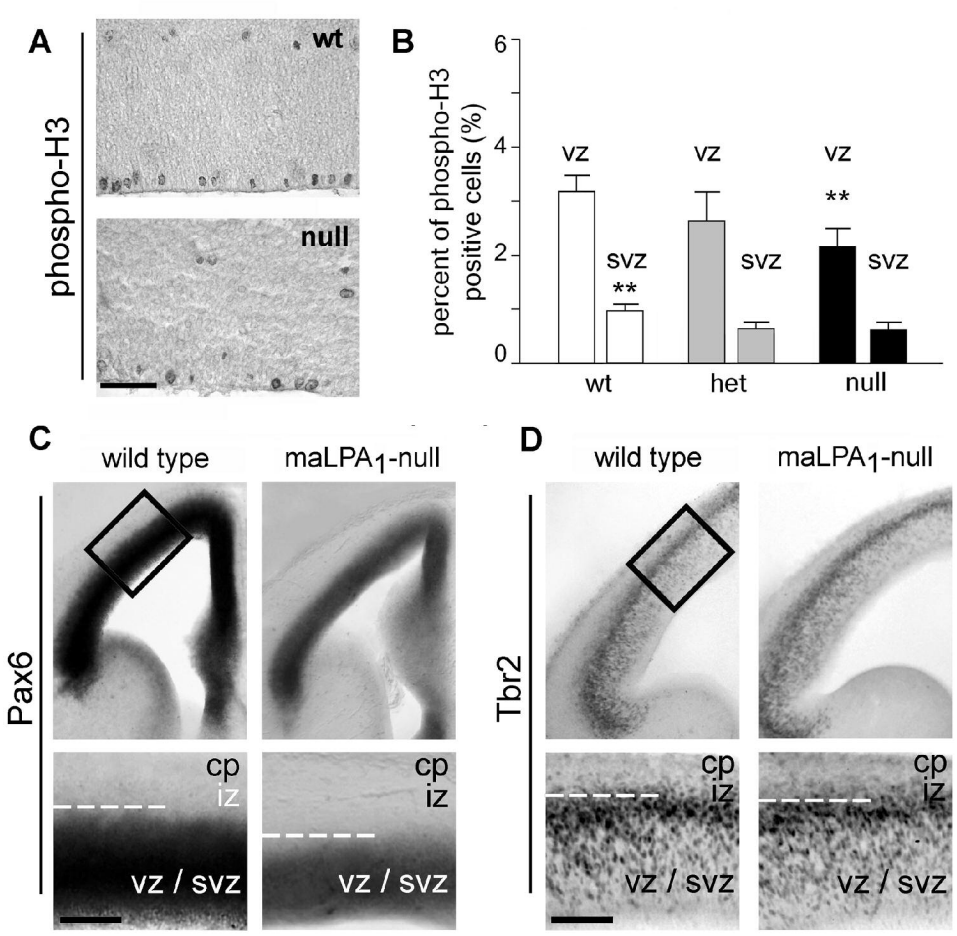

127x123mm (350 x 350 DPI)

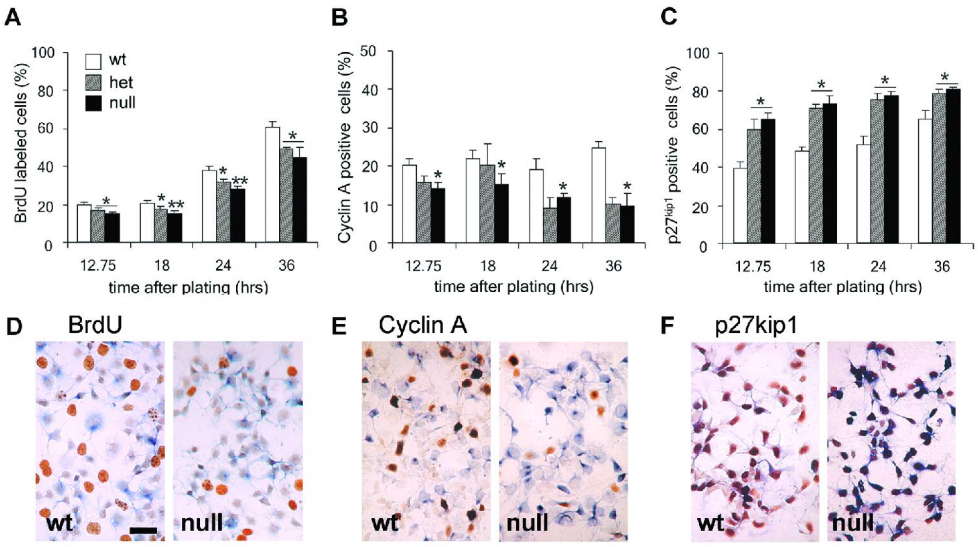

175x100mm (300 x 300 DPI)

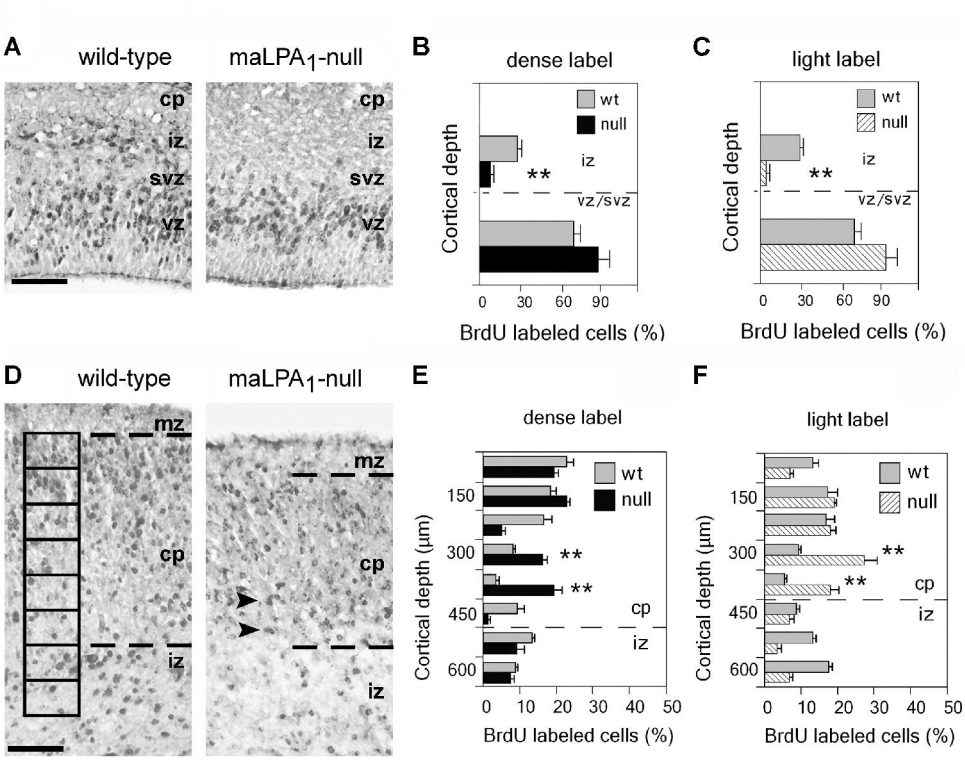

163x127mm (400 x 400 DPI)

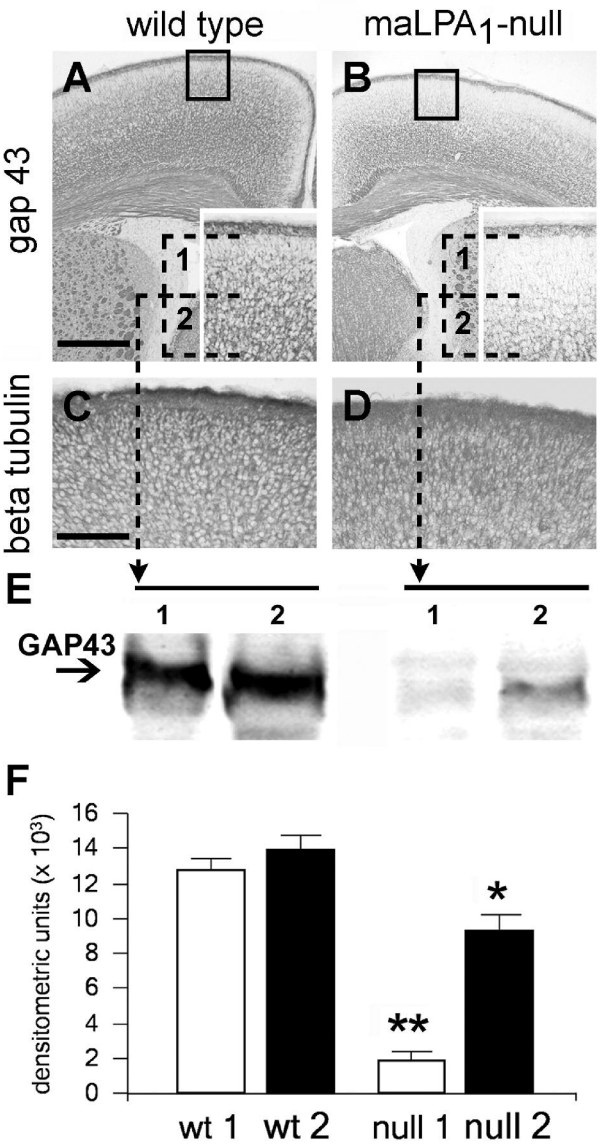

77x126mm (600 x 600 DPI)

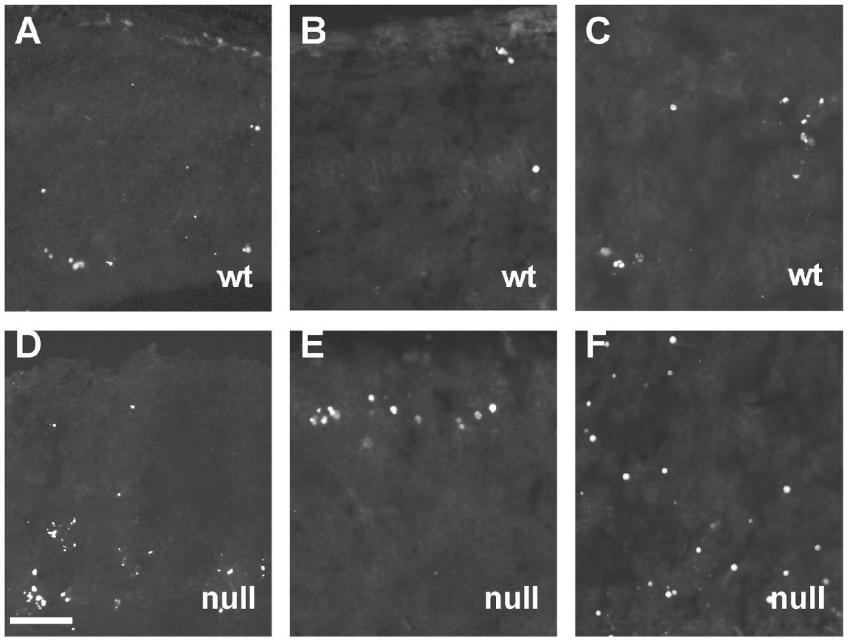

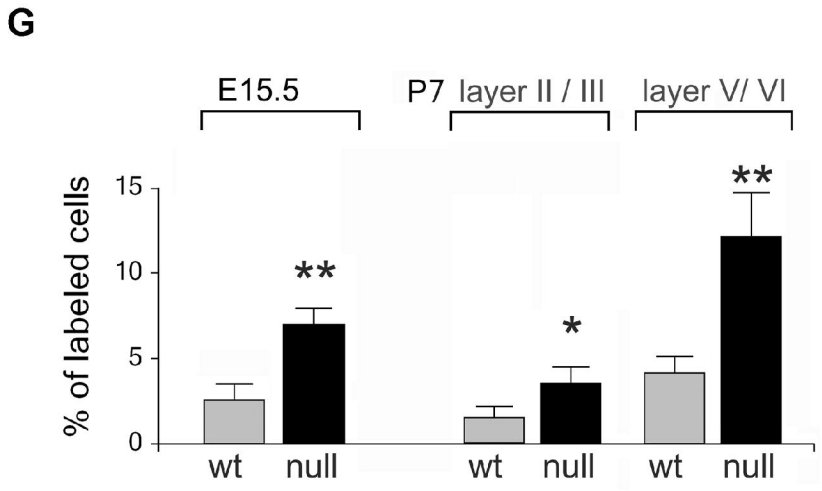

98x134mm (400 x 400 DPI)

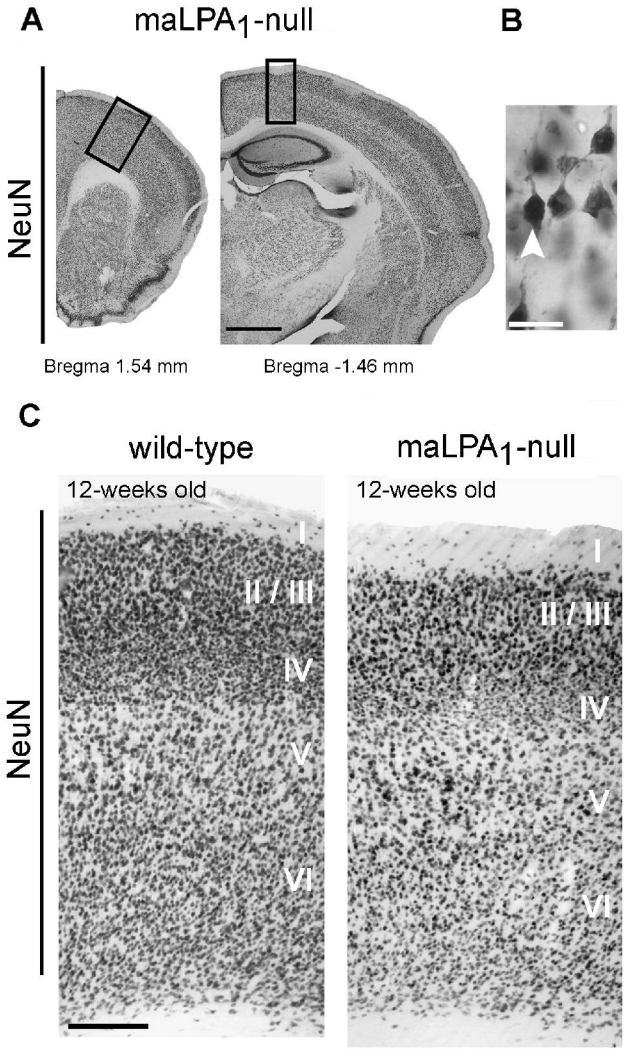

85x160mm (400 x 400 DPI)

Supplementary Table 2
Summarized comparison between reported LPA_1-null mice and the *Malaga* variant, $maLPA_1$-null mice

LPA_1-null		$maLPA_1$-null
Phenotype		
viability and fertility	semi-lethal, fertile	viability > 95% , fertile
suckling behavior	impaired	normal
olfactory capability	impaired	variable ; reduced olfactory bulbs
gross body anatomy		
decreased postnatal growth rate	yes	yes
reduced size	yes	yes
craniofacial dysmorphism; shorted snouts	yes	yes
Low incidence of facial frontal haemotoma	2.5%	< 3%
Nervous system analysis		
Apoptosis of Schwann cells from sciatic nerve	increased	not tested
Cerebral wall thickness / brain size	variable reduction	always reduced
Developmental defects in neurogenesis	not observed	reduced proliferation; increased apoptosis Early expression of neuronal markers
Postnatal defects	not observed	increased apoptosis; loss of cortical cellularity GAP43 deficiency
Response to LPA in dissociated neuroblasts		
impaired clustering	yes	yes
Decreased proliferation	yes	yes

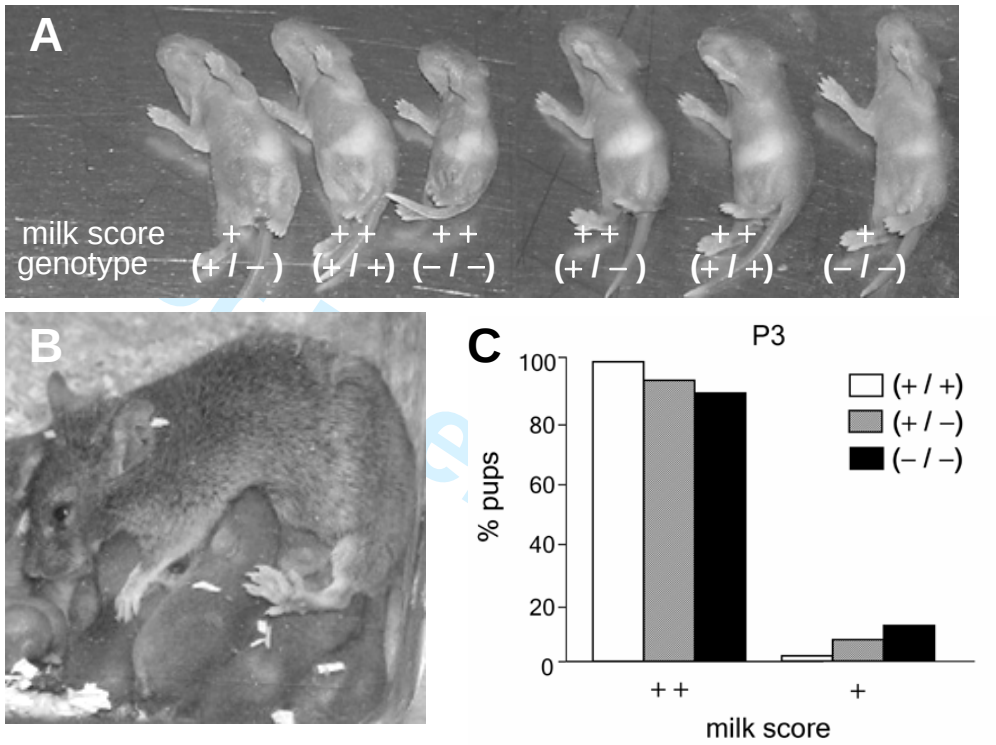

Supplementary figure 1. Suckling defects are not observed in neonatal maLPA$_1$ null mice. ***A***, Only few pups exhibit partial reduction of milk in stomachs of ma*lpa*$_1^{(-/-)}$ and ma*lpa*$_1^{(+/-)}$ P3 mice as compared with their wild-type ma*lpa*$_1^{(+/+)}$ littermates. Relative abdominal milk was estimated either as full / near full (+ +), intermediate (+), or empty/ near empty as previously reported by Contos et al. 2000. ***B***, Normal suckling behavior observed for ma*lpa*$_1^{(-/-)}$ × ma*lpa*$_1^{(+/-)}$ progeny. ***C***, Pup milk scores at P3 for ma*lpa*$_1^{(-/-)}$ and their corresponding ma*lpa*$_1^{(+/-)}$ and ma*lpa*$_1^{(+/+)}$ littermates showing the predominant occurrence of normally near full stomach . Only a minor percentage had a tendency to display an intermediate score (n = 26) but not presenting statistical significance.

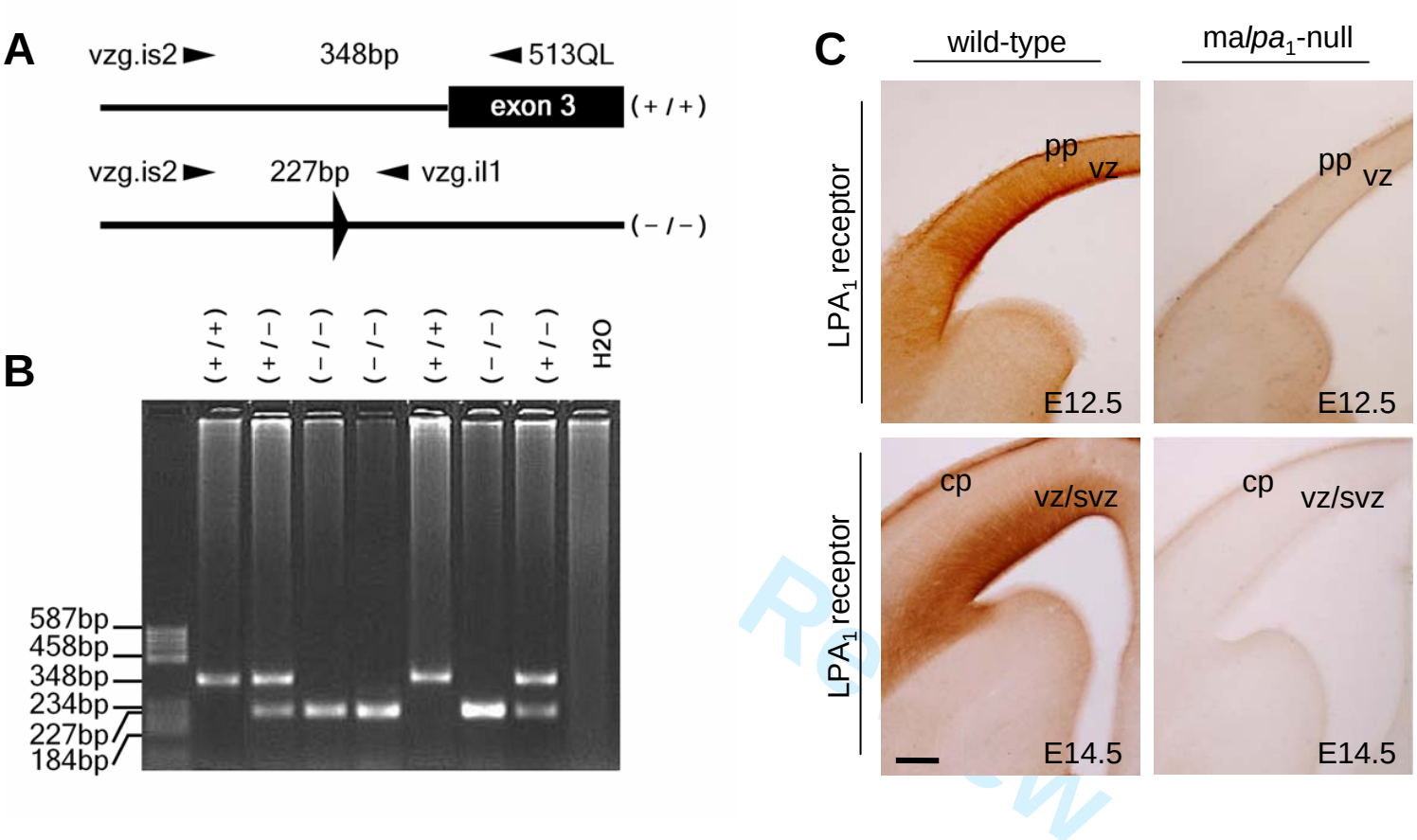

Supplementary figure 2.

A, ***B***, PCR assay for genotyping of mice. ***A***, Scheme of PCR assay for detection of wild-type *lpa1* (348bp) inheritance and targeted deletion (227 bp) according to Contos et al. 2000 in *Malaga* variant, named as ma*lpa*$_1$. ***B***, Expected product sizes were obtained with genomic DNA (50-100 ng/ µl/ reaction) added as a template in a 50 µl PCR (35 cycles of 95ºC for 30 s, 56ºC for 30 s, and 72ºC for 2 min, with a final incubation of 72ºC for 5 min before cooling to 4ºC) containing BioThermMix™ reagent (Genecraft GmbH) and the following three primers: 513QL (5'-GCCAATCCAGCGAAGAAGTC-3'), vzg.il1 (5'-GGTATTCTTAATTCTAGAGGATCA GC-3'), and vzg.is2 (5'-TATAGGAGTCTTGTGTTGCCTGTCC-3').

C, Immunolocalization of LPA$_1$ expression in E12.5 and E14.5 coronal sections from the cerebral cortex of wild-type and malpa1-null embryos. The expression of LPA$_1$ receptor appeared confined to neurogenic VZ/SVZ proliferative zones. CP, cortical plate; PP, preplate; VZ, ventricular zone; VZ/SVZ, ventricular plus subventricular zones. Scale bar in (*C*, E12.5), 450 µm;(*C*, E14.5), 150 µm

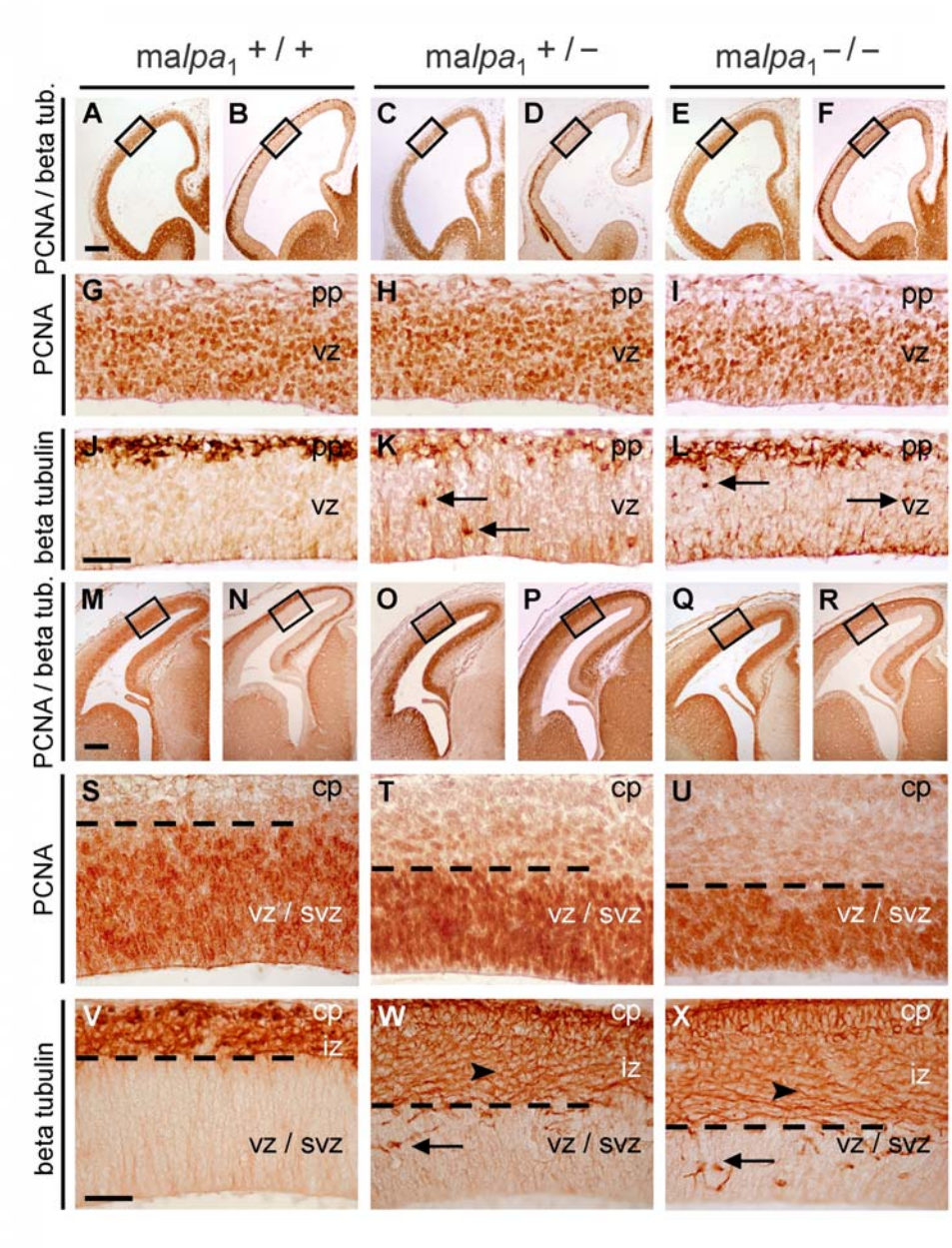

Supplementary Figure 5.
Cortical proliferative patterning is affected in mice lacking LPA_1. Original plate.
Expression patterns of PCNA and beta-tubulin-III in E11.5 sagittal (***A-L***) and E14.5 coronal (***M-X***) sections from the cerebral cortex of wild-type (***A, B, G, J, M, N, S, V***), ma*lpa*$_1$ heterozygous (***C, D, H, K, O, P, T, W***) and ma*lpa*$_1$-null (***E, F, I, L, Q, R, U, X***) embryos. By E11.5 the absence of *lpa*$_1$ resulted in a slight reduction of PCNA immunoreactive area (***I***) and early expression of beta-tubulin-III in VZ cells (arrows in ***K*** an ***L***), predominantly next to the ventricular surface. At E14.5, an anomalous germinative layering resulted when the receptor was absent in comparison with wild-type patterning, demonstrated by a reduction of PCNA in VZ/ SVZ and a premature strong expression of beta-tubulin-III in that area (arrows in ***W*** and ***X***). At this age beta-tubulin-III immunodetection showed a disturbance in cortical radial organization with fibers running parallel to ventricular surface (arrowheads in ***W*** and ***X***). Broken lines delimit marker expression. Depicted squares (*A-F, M-R*) are magnified 10x in the next images. CP, cortical plate; IZ, intermediate zone; PP, preplate ; VZ, ventricular zone; VZ/SVZ, ventricular plus subventricular zones. Scale bars in (A-F), 250 µm; (*G-L*), 55 µm; (*M-R*), 300 µm; (*S-X*), 65 µm.

INSTITUTO MEDITERRÁNEO PARA EL AVANCE DE LA BIOTECNOLOGÍA Y LA INVESTIGACIÓN SANITARIA
IMABIS

Dr. Pasko Rakic

Cerebral Cortex

Málaga, June 8th 2007

Dear Dr Rakic,

According to your suggestions, we are sending to you a revised version of the manuscript entitled "Absence of LPA1 signaling results in defective cortical development" (REF. CerCor-2007-00088) to be published in *Cerebral Cortex*.

As required by the reviewers, we have included new experimental data and discussion in order to address their main concerns, clarify topics, and improve the quality of the article. We are sending you a copy of the original submission with the corrections included.

Concerning the remarks of the two reviewers:

Reviewer #1

1. – A section comprising of discussion and a major conclusion of observed alterations in the angle of cleavage plane has been added, including a reasonable update of the main literature concerning cell division, SVZ progenitors, and the cleavage plane.

2. – Likewise, *in vitro* work performed by Dr Chun's research group has been considered in the discussion of results.

Both topics have been included in the discussion, as suggested, and we hope they clarified this new version.

Avda. Carlos Haya, 82; Pabellón A, planta 7; Málaga 29010. SPAIN; Tel: 34 951 290 346; Fax: 34 951 291 447

INSTITUTO MEDITERRÁNEO PARA EL AVANCE DE LA BIOTECNOLOGÍA Y LA INVESTIGACIÓN SANITARIA
IMABIS

Reviewer #2

1. – A supplementary figure 2 has been extended, adding LPA_1 immunostaining performed on wild-type and $maLPA_1$-null embryos in order to specifically show the presence or absence, respectively, of LPA_1 for signaling. Thus, as suggested, a cellular compaction assay that shows the presence of LPA_1 in cells has been removed from Figure 4.

2. – We agree that variation in stomach content appeared confusing. Suckling defects in $maLPA_1$-null pups (Sup. Fig. 1) were cautiously measured and cautiously showed given that no statistical significance was expressed in the milk score histograms (Sup.Fig.1,C) of the initially submitted Supplementary Figure 1. Accordingly, in that figure the milk score of most of the born mice, whatever their genotype, was normal and it was also confirmed from the *in vivo* observation of suckling behavior within the litter. A slight percentage of $maLPA_1$-null pups showed a tendency to exhibit stomachs with less amounts of milk. That tendency was not observed in wild-type mice and was practically non-existent. This was what we expressed as "partially suckling defects."

   In order to avoid confusion the text has been rewritten expressing clearly the absence of suckling defects in $maLPA_1$-null mice, that is, the real fact, and specifying the mentioned tendency.

3. – Figure 2 has been converted into a false color mode to highlight the expression of each marker. After using several combinations of colored plates we finally agreed to use a blue-pattern on black background for a better visualization of the immunoreaction. Likewise, the original color figure has been added as a new Supplementary figure 5 in case of the original immunostaining may be required for any reader. Differences between each genotype, particularly those referred to in panels G-I, are now more understandable. However, we consider it significant to mention that $maLPA_1$-null embryos displayed just a slight reduction of PCNA expression at earliest ages (E11.5) whilst most remarkable observations were found in the beta tubulin III expression.

Avda. Carlos Haya, 82; Pabellón A, planta 7; Málaga 29010. SPAIN; Tel: 34 951 290 346; Fax: 34 951 291 447

INSTITUTO MEDITERRÁNEO PARA EL AVANCE DE LA BIOTECNOLOGÍA Y LA INVESTIGACIÓN SANITARIA
IMABIS

4. –Coincidentally, the suggested discussion of results now reports the extensive observed results concerning mitosis, apoptosis, angle of cleavage plane, cell division, and SVZ progenitors, which takes into consideration the recent literature in the field. This should clarify the sequence of events in absence of the LPA_1 receptor.
Likewise, the analysis of SVZ includes new data for Tbr2 expression that it has been incorporated in the text and figure 3. As reported in the text, no significant differences were found in Tbr2 expression. Based on Tbr2 studies (Englund et al 2005; Quinn et al 2007) a proliferative population of VZ/SVZ wild-type cortex, under normal circumstances, express a "Pax6 – Tbr2 – Tbr1" sequence parallel to the differentiation of apical progenitor cells into intermediate basal SVZ progenitors. The MaLPA1-null cortex exhibited a non-proliferative population of cells (assumed SVZ) with normal expression of Tbr2. From our results we conclude that both the Tbr2- and early aberrant beta-tubulin-III- expressing region are indicative of prematuration and are understood as an early decision to exit into the subsequent step, i.e. intermediate progenitor. These considerations have been included in the text.

5. – Concerning the suggestion to include the actual numbers of BrdU cells, we would like to make note of our intention when expressing percentages of BrdU cells. Thus, percentages of BrdU cells in figure 5 express the percentage of participation, obtained from the percentage of the total number of labeled cells in the strip (Gillies and Price 1993), not percentages of total cells labeled and unlabeled in the strip. That way, 30% BrdU lightly labeled in a bin of 200 microns depth means that 30% of all lightly labeled cells are occupying that position, being this a value independent of unlabeled cells and density and only valid for the examination of migration of a labeled population. Total cell number in SVZ and CP were not estimated. BrdU percentages are, effectively, "just percentages of BrdU+ cells affected, with total cell number comparable among mutants and wild-types."

6. – We agree that Figure 8 is somewhat confusing. The original figure 8 was not created to compare wild-type vs. null cortex, but to show what we consider the motor cortex in its rostro-caudal extension. However, we agree that in that way it does not appear to add anything substantial and it has been changed. Also, the figures have been properly labeled.

Avda. Carlos Haya, 82; Pabellón A, planta 7; Málaga 29010. SPAIN; Tel: 34 951 290 346; Fax: 34 951 291 447

INSTITUTO MEDITERRÁNEO PARA EL AVANCE DE LA BIOTECNOLOGÍA Y LA INVESTIGACIÓN SANITARIA
IMABIS

7. – MaLPA$_1$-null mice vs. founder LPA$_1$-null mice. This comment underscores a really interesting and very long-term issue that is at the forefront of modern genetics: the role of modifiers in affecting mutant phenotypes. There are literally scores of reports now in the literature that report the effects of UNKNOWN modifiers on a single mutant allele, the most prominent examples being the effects of background strain on mutant phenotype. Well known examples that affect the brain include caspase deficient animals as well as the *Orl* allele of Reeler [1-4]. In both of these cases, and the vast majority of reported strain-dependent differences, the full range of modifiers are not known. Identifying them represents an enormous undertaking, since it is usually done through positional cloning after enormous, time-consuming, and expensive back-cross analyses. Modifiers could be other genes, viruses, retrotransposons, etc., and finding them and proving their function is a major undertaking. Thus, the question of "why," which really means "how," is answered by stating that one or more genetic modifiers, occurring spontaneously, has produced the Malaga variant phenotype reported here. The suggestion to cross the Malaga variant with the original mice will not address the nature of the modifier(s). Even if an intermediate phenotype were observed, that does not allow conclusive statements to be made about the identity of the modifier, an issue vastly complicated by the variable phenotypes of the original LPA$_1$-null mice, in which 50% died perinatally. The fact that a highly penetrant and reproducible phenotype occurs in this Malaga variant should serve as a starting point towards understanding and identifying interacting genes or non-gene elements in future studies.

[1] Leonard JR, Klocke BJ, D'Sa C, Flavell RA, Roth KA. Strain-dependent neurodevelopmental abnormalities in caspase-3-deficient mice. J Neuropathol Exp Neurol. 2002 Aug; 61(8):673-7.
[2] Bergren SK, Chen S, Galecki A, Kearney JA. Genetic modifiers affecting severity of epilepsy caused by mutation of sodium channel Scn2a. Mamm Genome. 2005 Sep; 16(9):683-90.
[3] Nadeau JH. Modifier genes in mice and humans. Nat Rev Gen. 2001 Mar; 2(3):165-74.
[4] Rice DS, Curran T. Role of the reelin signaling pathway in central nervous system development. Annl Rev Neurosci 2001; 24:1005-39.

We believe this revision and response address adequately the critiques of the reviewers. We are looking forward to hearing from you.

Yours truly

G. Estivill Torrús

For the authors

Avda. Carlos Haya, 82; Pabellón A, planta 7; Málaga 29010. SPAIN; Tel: 34 951 290 346; Fax: 34 951 291 447

Supplementary Table 1
Inheritance of the ma*lpa*1 deletion allele

	Litter genotypes			
Parental genotypes	+ / +	+ /–	– /–	Expected – /–
At weaning (approximately P21)				
+/+ × +/–191 (49%)	198 (51%)	0 (0%)	0	
+/– × +/–	80 (28%)	141 (50%)	61 (22%)	70
+/– × –/–	0 (0%)	193 (55%)	159 (45%)	193
Sex ratios (female:male)	131:140	254:278	99:121	
Embryonically (E14-E18)				
+/+ × +/–	35 (49%)	37 (51%)	0 (0%)	0
+/– × +/–	21 (26%)	41 (51%)	19 (23%)	21
+/– × –/–	0 (0%)	36 (52%)	33 (48%)	36

Analysis of genotyped offspring is shown for the specified matings (P, postnatal day; E, embryonic day). Data are expressed as numbers of individual progeny and percentage of each genotype (in parentheses as rounded to the nearest percent). Results show a slight proportion of ma*lpa*1 (– / –) null mice lost after birth.

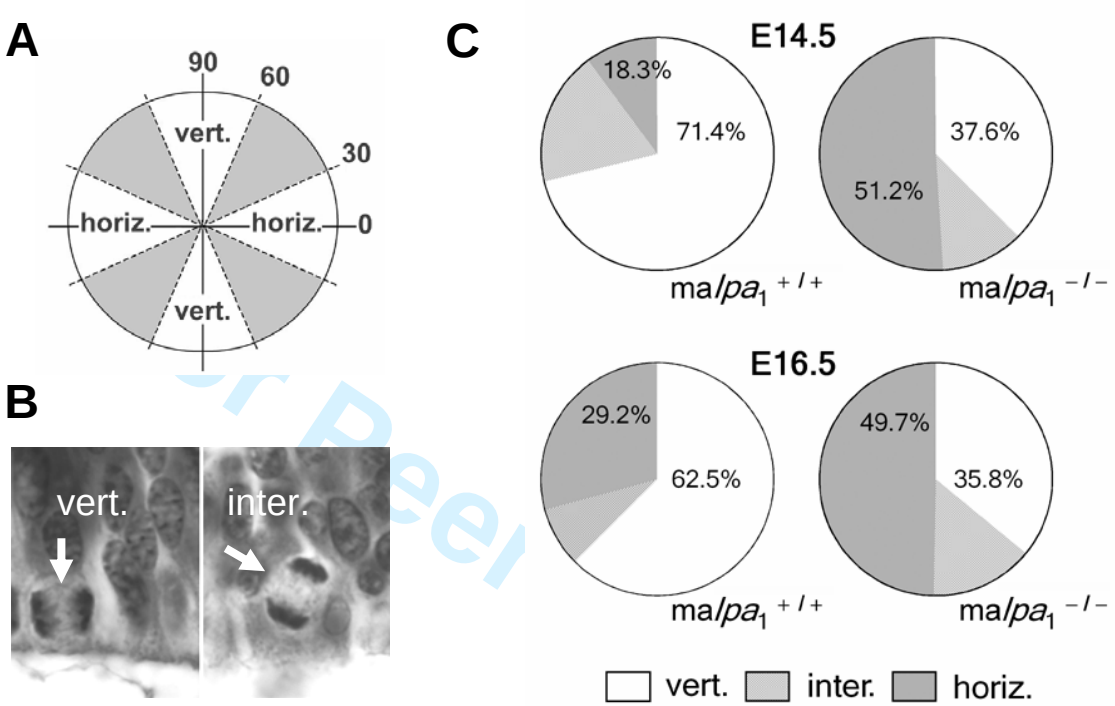

Supplementary figure 3. Absence of LPA_1 in neural precursors correlates with altered plane of division. ***A***, Late anaphase and telophase cells were classified by their plane of division relative to the ventricular surface (0°): –30° to 30°, horizontal cleavage; 30° to 60°, intermediate or oblique division; 60° to 120°, vertical cleavage. ***B***, Hematoxylin illustrates labeled chromosomes showing vertical (left) and intermediate (right) cell divisions. Arrow indicates plane of cell division. ***C***, Graphs comparing the percentage of dividing cells undergoing vertical, intermediate and horizontal division (identified in cross sections) in ma*lpa*$_1$ (+ / +) and ma*lpa*$_1$ (– / –) embryos at E14.5 and E16.5 stages. Wild-type proportions of vertical and horizontal division are markedly inverted in the maLPA$_1$-null cortex and maintain as brain develops (n = 8; $p < 0.001$).

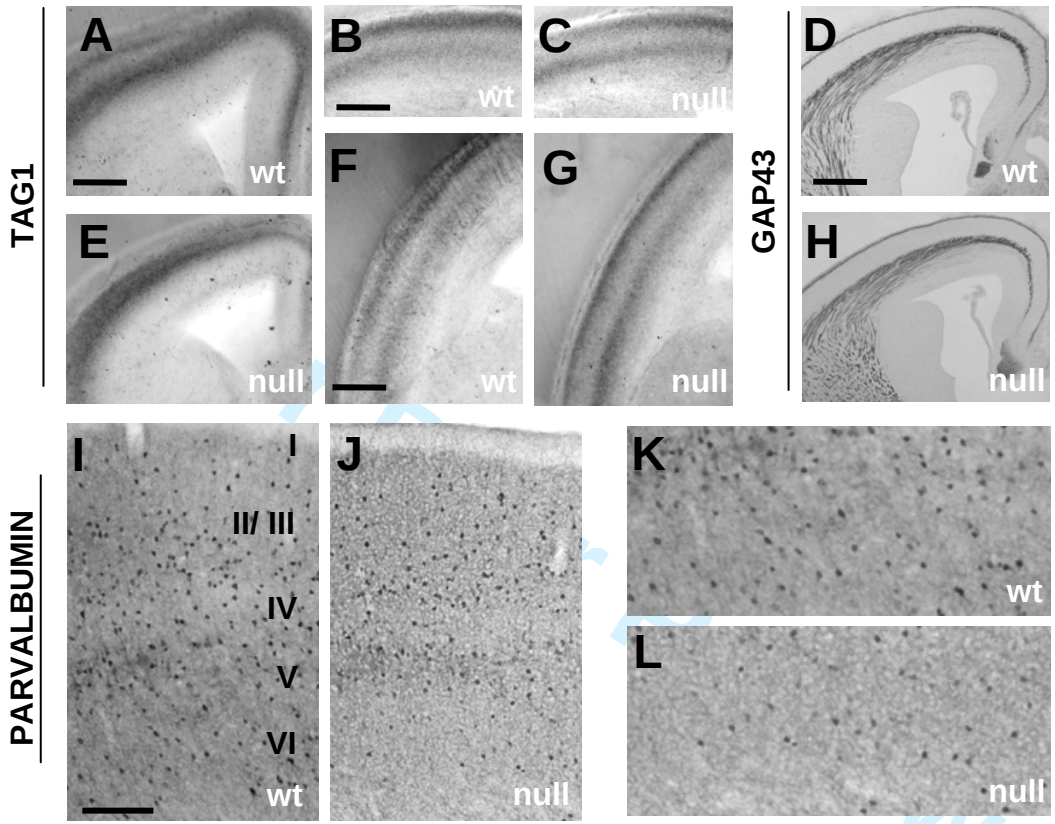

Supplementary figure 4. Cortical lamination in mice lacking LPA_1 receptor. ***A-C, E-G***, In situ hybridization for TAG1 expression on coronal brain sections from E14.5 (*A, E*) and E17.5 (*B, C, F, G*) wild-type (wt) (*A, B, F*) and homozygous $maLPA_1$-null mutant (null) (*C, E, G*) littermates. *D, H*, Immunohistochemical analysis of GAP43 expression for same embryos. Both, TAG1 and GAP43 studies showed no evidences for defective tangential migration or corticofugal axonal pathways when LPA_1 is absent. ***I-L***, Analysis of parvalbumin positive neurons by immunohistochemistry on cerebral coronal sections from 12-week old mice. A reduction of neuronal population is generally observed, particularly affecting cortical layers V and VI (*K, L*), in absence of LPA_1 (*J, L*) as compared with wild-type cortex (*I, K*). Scale bars in (*A, B, C, E, F, G*), 300 µm; (*D, H*), 350 µm; (*I, J*),200 µm; (*K, L*) 2x magnified from (*I, J*).